

NASA Technical Memorandum 87686

INFRASONIC EMISSIONS FROM LOCAL METEOROLOGICAL
EVENTS: A SUMMARY OF DATA TAKEN THROUGHOUT
1984

ALLAN J. ZUCKERWAR

FEBRUARY 1986

(NASA-TM-87686) INFRASONIC EMISSIONS FROM
LOCAL METEOROLOGICAL EVENTS: A SUMMARY OF
DATA TAKEN THROUGHOUT 1984 (NASA) 50 p
HC A03/MF A01 CSCL 20A

N86-21281

Unclas
G3/71 05625



NASA

National Aeronautics and
Space Administration

Langley Research Center
Hampton, Virginia 23665

INTRODUCTION

Throughout the year 1984, records of infrasonic signals propagating through the Earth's atmosphere in the frequency band 2-16 Hz were gathered on a three-microphone array at Langley Research Center. The accumulation of these records was motivated by the need to develop a technique for locating and identifying natural sources of infrasound, such as local and distant meteorological events, for potential application in a low level wind shear alert system.

Past investigations of natural sources of infrasound have focused on severe storms and clear air turbulence (refs. 1-6). Most of the experimental observations were obtained using the microbarograph and were limited to frequencies below about 0.1 Hz. The observations of reference 6, on the other hand, used microphones in the range 1-16 Hz, about the same as used here, but again the study emphasized correlation of infrasound with clear air turbulence, and the array was too small for accurate source location. The present investigation is based on the assertion that local meteorological events, such as microbursts, are also effective emitters of infrasound, and that the emissions can be used for the purpose of source location and identification.

The purpose of this memorandum is to document the supporting evidence of those cases where the infrasound received by the array is believed to have originated from a local meteorological event like a microburst. It consists of (1) a description of the infrasonic detection system and the data processing procedure; (2) a classification of received infrasonic signatures and their relationship to both global and local meteorological events; and (3) the potential role of the infrasonic array in a practical wind shear alert system.

INFRASONIC DETECTION SYSTEM

Layout of the Array

The microphone array is located in an open field near the Landing Loads Facility at Langley Research Center (fig. 1). The nature of the terrain dictates the array shape to be an isosceles rather than an equilateral triangle, having the dimensions shown in the figure. The size of the array is determined by a compromise between good bearing resolution and data file size. Three microphones are sufficient to locate a source unambiguously from measurement of the received infrasound.

Suppose an infrasonic wave approaches a microphone pair located at positions A and B shown in figure 2. The time delay τ_{AB} is the time required for the wavefront to travel between the two microphones:

$$\tau_{AB} = (d/c) \cos \theta, \quad (1)$$

where c is the sound speed and d the distance between microphones. If the microphone signals are digitized at time intervals Δt , then the bearing resolution -- the uncertainty in the angle θ corresponding to an uncertainty of one sample interval -- is found to be

$$\Delta\theta = c\Delta t/d \sin \theta \quad (2a)$$

At large angles of incidence ($\theta \approx 90^\circ$) this can be approximated by

$$\Delta\theta = 90^\circ - \cos^{-1}(c\Delta t/d), \theta \approx 90^\circ \quad (2b)$$

and at small angles of incidence ($\theta \approx 0^\circ$) the uncertainty in angle is limited by the uncertainty of one time resolution:

$$\Delta\theta = \cos^{-1}(1 - c\Delta t/d), \theta \approx 0^\circ \quad (2c)$$

The bearing resolution deteriorates strongly with decreasing array spacing d . The data file size D_{\max} is the number of samples required to record signals over the maximum delay. The required maximum file size corresponds to propagation along the microphone axis A-B. In this case

$$D_{\max} = \tau_{AB-\max}/\Delta t + 1 = d/c\Delta t + 1$$

However, as is shown in reference 7, the capability of obtaining lag-lead information requires that only alternate data points be used to find the delay. This requirement essentially doubles the data file size:

$$D_{\max} = 2d/c\Delta t + 1 \quad (3)$$

The bearing resolution and data file size, computed from equations (2a) and (3) for three different microphone separations, are shown below:

TABLE 1.- MICROPHONE SEPARATION VERSUS DATA
FILE SIZE AND BEARING RESOLUTION

Microphone separation d , ft	2000	800	100
Data file size, samples	200	77	10
Bearing resolution $\Delta\theta$	0.85°	2.1°	17.1°

The computations are based on a sound speed $c = 1080$ ft/sec, sample interval $\Delta t = 1/51.2$ sec (see "Signal Processing"), and typical angle of incidence $\theta = 45^\circ$. A large array affords fine bearing resolution at the expense of large data file size; for a small array the reverse is true. The choice of $d = 800$ ft yields reasonable values for both criteria in the present system.

In order that the microphones provide continuous service in the field, they are enclosed in fibrous windscreens and are weather-protected by partially open wooden shelters. Their cables run into an instrumentation van located within the array. The operating system, being fully automatic, is left unattended, except for a daily visit by an operator to replace the data storage disk if the latter is full.

Instrumentation

Figure 3 shows a block diagram of the instrumentation.

Microphones.— The infrasonic pressure sensors are Globe 100C Capacitor Microphones, manufactured by Gus Manufacturing, Inc., El Paso, Texas. These microphones feature a large membrane diameter (2 1/4 in.) and pulse-width-modulated carrier electronics, permitting high sensitivity and response to very low frequencies. The essential specifications are given in table 2:

TABLE 2.— ESSENTIAL SPECIFICATIONS OF GLOBE 100C CAPACITOR MICROPHONES

Open-circuit sensitivity ^a	400 mV/Pa
Frequency response (-3 dB)	0.1-500 Hz
Maximum undistorted signal level	± 10 V (119 dB SPL) ^b
Equivalent noise (0.1 - 500 Hz)	± 2 mV (45 dB SPL)

^a"Low" sensitivity setting.

^bSPL = rms sound pressure level referred to 20 μ Pa.

The microphones are periodically calibrated in the field by the pistonphone technique at a SPL of 104.7 dB and frequency of 250 Hz.

Amplifiers-attenuators.— For the gathering of weather-related infrasound these were set at 20 dB gain, which raises the noise floor and lowers the maximum undistorted signal level.

Filters.— The infrasonic passband was initially set at 0.1-20 Hz, but after some preliminary measurements, was changed to 2-16 Hz for the following reasons. The infrasonic background below 1 Hz was found to be incoherent and dominated by the wind. The windscreens proved only partially effective in reducing wind-induced pressure fluctuations at the microphones. In order to minimize the masking of propagating infrasonic signals by the background, it was decided to reject all signals below 2 Hz. This limiting frequency was adjusted both acoustically, by shortening the vent tube used for pressure equalization in the microphone backchamber, and electronically by means of a 2-pole highpass Butterworth filter. The choice of upper limiting frequency was dictated by the sampling frequency, as will be explained below.

The lowpass filter is a 6-pole Bessel filter, chosen for optimal phase fidelity. By lowering the upper cutoff frequency from 500 to 16 Hz, the filter reduces the noise floor by a factor $16/500 = -30$ dB.

A/D converter.— The A/D converter is an AI13 Analog Input System, manufactured by Interactive Structures, Inc., Bala Cynwyd, PA. The essential specifications are listed in table 3:

TABLE 3. ESSENTIAL SPECIFICATIONS OF AI13 ANALOG INPUT SYSTEM

Number of bits	12 (4096 steps)
Full scale voltage range	± 5 V (selected from among 8 ranges)
Bit resolution	2.44 mV
Maximum number of channels	16
Conversion time	20 μ sec

Because the full scale output voltage, ± 5 V peak-to-peak, is a factor of 2 smaller than that of the microphone, the upper limit to the dynamic range falls another 6 dB. Further, the conversion time is much faster than actually needed, since only 3 of the 16 channels are being multiplexed.

A summary of contributions to the net dynamic range of the infrasonic instrumentation system is given in table 4:

TABLE 4.— CONTRIBUTIONS TO THE DYNAMIC RANGE

	<u>Lower limit</u>	<u>Upper limit</u>
Microphone	45	119 dB
Amplifier-attenuator	20	-20
Filter	-30	0
A/D converter	<u>0</u>	<u>-6</u>
Net dynamic range	35	93 dB

Microcomputer.— Despite limitations on data storage capacity and processing time, an Apple II computer with 48K of memory was chosen as the system processing unit to keep the cost low. The peripherals include two floppy disk drives, a thermal printer, and a memory card to increase the memory to 64K. A modem could be added for communication between two systems over commercial telephone lines.

Signal Processing

The signal processing routines fulfill three functions: time delay estimation (TDE), source location, and source identification. The "time delay estimation" routine, running in real time, applies criteria as to whether or not a sampled time history will be saved on disk and, if affirmative, computes time delays between microphone pairs. The "source location" routine determines the location of the source from the measured time delays between the three microphone pairs. The "source identification" routine is based on the computation of power spectra in the frequency domain.

Time delay estimation routine.— A flow diagram for the TDE routine is shown in figure 4. After the time histories of the three microphones are digitized and entered into the computer, they are processed in an "adaptive filter" routine, which yields the time delay estimates (TDE's) among the three microphone pairs. However, not all time histories are accepted. The TDE's are subjected to two tests: a "variance test," relating to the quality of the signal, and a "consistent delays test," determining whether or not the microphone signals originate from a common source. If the measured TDE's pass both tests, then the time delays are printed and the time histories are saved on a floppy disk. Time histories are sampled and tested repeatedly until the floppy disk fills up.

(i) Input time history. The analog infrasonic signals received by the microphones are sampled by the A/D converter and stored in computer memory. The sample rate was chosen to be 51.2 samples/sec. This is 3.2 times the cutoff frequency of the lowpass filter and made somewhat in excess of the Nyquist frequency because of the slow rolloff of the Bessel filters. Furthermore, this sample rate produces exact frequency increments of 0.2 Hz on a 256-point Fast Fourier Transform (FFT) spectrum.

The inputted time histories are organized into files, each containing 8 blocks of 128 samples. Thus each file contains $8 \times 128 = 1024$ sampled points, representing a time window of $1024/51.2 = 20$ sec. One side of a floppy disk can hold a maximum of 16 files, each containing three channels.

(ii) Adaptive filter. Time delay estimates of signals corrupted by background noise are invariably based on cross correlation, either in the time domain or frequency domain. In the time domain, for example, the estimate is determined from the time delay at which the cross correlation function peaks. However, the finite time window of the sampled signal and the presence of uncorrelated noise cause spreading of the correlation peak and an error in the time delay estimate. A common countermeasure to minimize the effect of the spreading error is to use a weighting function in the computation of the cross correlation function. In the present application this procedure leads to two major difficulties. First, weighting functions, as used in the past, require time-consuming computations in the frequency domain. Secondly these weighting functions require a prior knowledge of the frequency spectrum of the received signal. In the passive detection system described here this information is unknown.

The adaptive filter used here is designed to overcome these difficulties. The filter, described in detail in reference 7, features (1) a self-optimizing weight selection, so that a prior knowledge of the signal is unnecessary, and (2) an analysis confined to the time domain, so that transformation to the frequency domain is completely avoided. Briefly, the time histories of a microphone pair are represented as a sequence of samples of record length L . Both microphones generally contain uncorrelated noise; but a propagating component at one microphone will also appear at

the second microphone, delayed by a time corresponding to a number of samples D . The samples of the first microphone are assigned weights, and the weighted samples are shifted by some delay and subtracted from the corresponding samples of the second microphone. The resulting differences make up an error function, which is then minimized with respect to the weights by a least-mean-squares algorithm. The minimization procedure leads to an updated set of weights, which are used to recompute the error. With successive iterations an optimum weighting function is ultimately reached, which shows a peak at the sample number corresponding to an optimum delay D . In the present filter the number of iterations is set equal to the record length L . The choice of $L = 128$ samples for the TDE easily exceeds the 77 samples required to cover the maximum delay. An example of the TDE's plotted against iteration number for the three microphone pairs is shown in figure 5.

(iii) Variance test. In a well designed filter the TDE of a coherent source will converge to its limiting value very rapidly with an increasing number of iterations. In practice, the TDE may fluctuate slightly about its limiting value due to the unavoidable influence of spurious, incoherent signal components. Some evidence of this tendency can be seen in figure 5. The TDE of a strongly incoherent signal will be so badly broken that it will not converge to an unambiguous limit. The evaluation of the TDE, then, must allow for some fluctuation, but must reject records yielding unacceptably poor TDE's. The criterion for acceptance of a record is that the TDE must lie within a preset tolerance (the "variance threshold" VT) over a given number of iterations (a sliding "variance window" K). After a period of trial and error the values $VT = \pm 5$ samples (out of ± 33) and $K = 48$ iterations (out of 128) proved effective in accepting records of suitable quality. In figure 5 the TDE lies within the variance threshold between iterations 36-128 for all three microphone pairs.

(iv) Consistent delays test. There is a remarkably simple test to determine whether the signals at the three microphones emanate from a single source. Suppose the propagation times from a source to the three microphones are τ_1 , τ_2 , and τ_3 respectively. Then the time delay estimates τ_{12} , τ_{23} , and τ_{31} , and their sum are the following:

$$\begin{aligned}\tau_{12} &= \tau_1 - \tau_2 \\ \tau_{23} &= \tau_2 - \tau_3 \\ \tau_{31} &= \tau_3 - \tau_1 \\ \hline \tau_{12} + \tau_{23} + \tau_{31} &= 0\end{aligned}\tag{4}$$

In other words, the sum of the three TDE's, properly permuted, must be zero if the signals emanate from a single source. In practice, to allow for sample error, a record is accepted only if the sum of the TDE's falls within ± 0.12 sec (about ± 3 digital increments). This test was not applied to data taken prior to September 12, 1984.

(v) Print delays. If a time history succeeds in passing the "variance" and "consistent delays" tests, then the time delays of the three microphone pairs are printed for subsequent processing in the "source location" routine (see below). The sign of the delay indicates lag or lead. The printout includes a "file number," assigned sequentially to the successful time histories, and an "attempt number," the running number of sampled time histories, both successful and unsuccessful.

(vi) Save time history. A successful time history is saved on a five inch floppy disk. A disk can accommodate 16 files, each containing the 1024-point time histories of the three microphone channels. After a file is saved the routine is directed to the beginning of the loop to input another time history. If the disk is full the program stops.

The TDE routine, on the average, inputs time histories at the rate of about 12 per hour. In other words the routine has a $1/12$ hr or 5 min processing time. Thus it inputs a 20 sec record every 5 min or 300 sec; that is, it samples the infrasonic environment $20/300 = 6.7\%$ of the time. This sample window is acceptable for the investigation conducted here. In a practical monitoring system, with more powerful computational hardware, it can be increased to about 70% of the time for a single array, as will be discussed below.

The "success rate," the ratio of the number of files saved on disk to the number of attempts, depends upon the choice of variance parameters in the variance test, the tolerance (in digital increments) in the consistent delays test, and the frequency of infrasonic activity. Obviously, too tight a variance threshold or too long a variance window would make the test overly restrictive and cause rejection of many signals from coherent sources. The final choices, $VT = \pm 5$ increments and $K = 48$ iterations, insure signals of suitable quality and duration for the present purpose, although these choices might not be optimal. The tolerance allowed in the consistent delays test, ± 3 time samples, is believed to be more restrictive in accepting files than the variance test. In one case of intense infrasonic activity as many as 11% of the inputted time histories were saved on disk. The disk filled up early, namely in $16/.11 = 145$ attempts or in $145/12 = 12$ hrs. At other times only 1% of the time histories were saved, requiring $16/.01 = 1600$ attempts over a period of $1600/12 = 133$ hrs or 5.5 days to fill the disk. Because the consistent delays test was first introduced on September 12, 1984, the success rate shows a substantial drop for subsequent data.

A summary of signal processing specifications is given in table 5.

After an operator replaces a filled data disk, he restarts the TDE routine, and processes the saved data afterwards with the "source location" and "source identification" routines.

Source location routine.— The determination of the source location is based on the following assumptions:

(1) Each file contains coherent signals from a single source. Coherent signals from more than one source will not allow the adaptive filter algorithm to converge.

(2) The source is stationary over the sampling period of 20 sec. As before, a nonstationary source will not allow convergence. Only the first 5 sec of the sampling period are used for the TDE; the remaining 15 sec are needed for later computation of power spectra.

TABLE 5. SUMMARY OF SIGNAL PROCESSING PARAMETERS

<u>Parameter</u>	<u>Original^a value</u>	<u>Proposed revision</u>
Array spacing d, ft	800	800
Bandwidth, Hz	2-16	2-20
Frequency resolution Δf , Hz	0.2	1
Time window per block T, sec	5	1
Number of spectral frequencies n_c	71	19
Block size N, samples	256	128
Time resolution Δt , sec	1/51.2	1/128
Sample rate f_s , samples/sec	51.2	128
Total time window T_d , sec	20	10
File length, samples	1024	1280
Number of averages per file n_d	4	10
Bearing resolution $\Delta\theta$	2.1°	0.85°
Acceptance angle $\Delta\theta'$	2.1°	4.3°
Standard deviation of bearing $\sigma(\theta)$	19.2°	7.3°
Acceptance probability P	8.5%	44.4%

^aThe original values given for block size N, total time window T_d , and number of averages per file n_d are used in the FFT (source identification) routine. For time delay estimation these values are changed to $N = 128$, $T_d = 5$ sec, and $n_d = 2$.

(3) The source is located near the ground and its emitted infrasound propagates parallel to the ground. If the source is in fact elevated, then the source location cannot be determined from the measured TDE's, but the TDE's can be corrected to yield the ground locations. However, the bulk of the data do not require this correction.

The source location routine is run on an independent computer after the data disk is collected from the instrumentation van. A flow diagram is shown in figure 6. The computation is carried out for all the files on the disk.

(1) Input time delays. The time delays are read from the TDE printout and entered into the computer through the keyboard.

(ii) Compute hyperbolic loci. For a measured time delay between two microphones, the locus of points representing all possible source locations defines a hyperbola. The microphones lie at the foci and the applicable branch of the hyperbola is determined by the lag-lead information. If the "consistent delays test," equation (4), is satisfied exactly, then the three hyperbolas corresponding to the delays among the three microphone pairs will intersect at a single point, which defines the source location. An example is shown in figure 7. If the test is only approximately fulfilled, then the hyperbolas will describe a small triangle representing the bounds of the source location.

If the source is distant, such that the infrasound propagates nearly as a plane wave sweeping across the microphone array, then the hyperbolas will have parallel asymptotes, pointing toward the source direction (fig. 8).

Sometimes the infrasound from a distant source bounces between the ground and the upper atmosphere, impinging upon the array at an angle ϕ relative to the ground plane. In this case the hyperbolic asymptotes will not be parallel, as shown in figure 9. The sound speed c of the wave propagating in the free atmosphere is related to the speed c_g of its propagation along the ground by

$$c_g = c \cos \phi \quad (5)$$

However, it is easily shown that reducing the time delays by $\cos \phi$ is equivalent to reducing the sound speed by $\cos \phi$. The result of reducing the delays of figure 9 by $\cos \phi = 0.707$ is shown in figure 10.

The routine prints the source locations (for local sources) and asymptotic directions (for distant sources) along with plots of the hyperbolic loci.

(iii) Input source location. The source coordinates or angles are read from the "compute hyperbolic loci" printout and entered into the computer through the keyboard.

(iv) Plot source location. The source location plot shows the locations of the sources relative to the array. An example is shown in figure 11. At locations beyond 5000 ft from center of the array, the bearing resolution is not adequate to distinguish between a local source or a distant source. This 5000 ft radius is indicated on the plot.

Source identification routine. This routine computes the cross power spectrum, auto power spectrum, and the coherence function of the time histories saved on disk. The computations are performed to investigate the possibility that local and distant meteorological sources can be identified by characteristic spectral signatures, if such exist. Like the "source location" routine, the "source identification" routine is run independently after the data disk is collected from the van. A flow diagram is shown in figure 12.

(i) Input time histories. The time histories are inputted under program control directly from the files saved on the data disk.

(ii) Compute cross power spectra. Cross power spectra are computed for microphone pairs 1-3 and 3-2 by a 256 point Fast Fourier Transform (FFT) routine and saved on a floppy disk. For computations in the frequency domain each file is divided into

4 blocks of 256 points, and each spectrum is the result of averaging 4 blocks of data. Upon completion of each computation the program provides a plot -- log cross power magnitude versus log frequency, best fits the computed magnitude to a straight line, and prints out the intercept, slope, and correlation coefficient of the straight line. If a spectrum can be described by a power law, then the slope is the exponent. The correlation coefficient indicates the goodness of fit. An example of the cross power spectra is shown in figure 13.

(iii) Compute auto power spectra. The auto power spectra for all three microphone channels are similarly computed and saved, plotted logarithmically, and fitted to a straight line. Several examples will be shown later.

(iv) Compute coherence functions. The coherence function $\gamma_{AB}^2(f)$ between the signals of two channels A and B is defined as

$$\gamma_{AB}^2(f) = \frac{|G_{AB}(f)|^2}{G_{AA}(f) G_{BB}(f)}, \quad (6)$$

where $G_{AB}(f)$ is the cross power spectrum, $G_{AA}(f)$ is the auto power spectrum of channel A, and $G_{BB}(f)$ is the auto power spectrum of channel B. This function ranges from unity, when the signals are from the same source, to zero, when they are completely uncorrelated. An example is shown in figure 14. The program inputs the cross and auto power spectra from the disks saved earlier, computes and plots the coherence function on a linear frequency scale (to facilitate identification of strongly coherent frequency components), and computes the average value of the coherence function for frequencies up to 12.8 Hz. The measured points are smoothed by plotting the average values of groups of four consecutive frequency components. As will be seen, the coherence function plays a crucial role in sorting out signatures from local meteorological events.

METEOROLOGICAL SUPPORT

Three sources of meteorological data at Langley Research Center greatly facilitate the correlation between meteorological events and infrasonic signatures.

National Weather Service.— "Significant meteorological advisories" (SIGMETS) are available continuously per teletypewriter from the National Weather Service. These advisories report and forecast the time, location, and windspeed of severe storms, and the location and severity of atmospheric turbulence -- the latter information often obtained from pilot reports ("PIREPS"). SIGMETS are used in the present study to track storms and to locate atmospheric turbulence.

Lightning locator plots.— A direction-finding system for locating lightning strikes operates at Langley Research Center in support of the Storm Hazards Program and the F106B Aircraft Storm Penetration Experiment. Antennas which detect the magnetic field due to a cloud-to-ground lightning discharge are situated at three stations in Virginia: Langley Air Force Base, Wallops Station, and Dahlgren (since moved to Charlottesville Airport). The direction-finding system locates each strike through triangulation, and transmits the data to a position analyzer, which maps the ground strike locations. The maps, called "lightning locator plots" (LLP's), also

contain the times of the first and last strikes and are available on a nearly daily basis. Figure 15 is an LLP showing strikes during thunderstorms north of Virginia on June 6, 1984.

Air weather service - surface weather observations (Form 10). - The weather station at Langley Air Force Base provides daily copies of this form to Langley Research Center. The form contains hourly readings of cloud cover, pressure, temperature, wind speed and direction, precipitation, etc., and thus provides a log of local weather.

INFRASONIC SIGNATURES AND THEIR RELATION TO METEOROLOGICAL EVENTS

Summary

The infrasonic detection system operated continuously in the automatic mode from June 6 to December 5, 1984. During this period data were gathered on 72 days, with some idle intervals for equipment and cable maintenance, power outages, holidays, etc.; 892 files were saved and analyzed out of an estimated 30 000 attempts. Although data were taken and saved manually as early as February 29, only data taken in the above period were subsequently analyzed.

A survey of the power spectra indicates that the overwhelming bulk of the files can be organized into four classes, based on the shape of the spectrum and on the magnitude of the coherence function over the experimental range of frequencies 2-16 Hz.

Class A spectra (both cross and auto) are characterized by a broad peak and high coherence. These are believed to originate from man-made sources. An example, a sonic boom from a military jet maneuvering in the vicinity of the array, is shown in figure 16. Altogether 136 saved files, or 15% of the total, belong to class A.

Class B spectra show one or more prominent discrete frequencies, which are believed to control the convergence of the adaptive filter (fig. 17). The prominent frequencies are usually in the vicinity of 10 Hz -- but on a rare occasion as low as 4 Hz, have a high coherence and high amplitude (at least 20 dB above the background), and occur according to no identifiable pattern. Although the source of these frequencies remains unknown, the heavy machinery used to operate the Langley wind tunnels and to test jet engines at Langley Air Force Base are possible candidates. Spectra of this class are the most common (62%), because in the absence of meteorological sources they appear with sufficient frequency to fill the disk. Nevertheless, in a practical infrasonic monitor these signals could be identified and deleted through software control, for it is unlikely that they have any relationship to the weather.

Class C spectra contain one or more narrow peaks, about 5 components wide, and have a high coherence across the peak (fig. 18). Although the source of these peaks lies predominantly at an angle of 167° with respect to the array (southeast), no attempt has been made to identify it. This class of spectra is relatively rare, occurring in only 68 or 7.6% of the saved files.

Class D spectra have two distinguishing features: (1) a good fit to a power law with a negative slope but (2) low coherence (<0.4) at nearly all frequencies

(fig. 19). This class of spectra is particularly interesting, because the associated infrasound is believed to emanate from meteorological events; it will be the subject of the remainder of this memorandum.

The occurrence of class D activity is distributed among the operating days as follows: On 36 or half the operating days no class D files were saved on disk; on 21 days (29%) there was little class D activity, 1-5 files; on 15 days (21%) there was moderate-to-strong class D activity, 6 or more files. Interestingly, it was discovered, after the spectral classification was completed, that each day showing moderate-to-strong class D activity also showed a major global meteorological event in or near the eastern United States, the lone exception being a day when severe turbulence was reported throughout this region.

Model of Weather-Related Infrasonic Sources

An interpretation of the class D signatures must take into account two contradictory facts: (1) The coherence between microphones is low, but (2) the adaptive filter routine assures convergence only for coherent signals. A model to resolve this paradox is based on the assertion that there are three distinct contributions to the infrasonic signal detected at each microphone: (1) fluctuations in ambient pressure due to turbulence -- the dominant contribution, which masks the other two, namely (2) infrasonic emission from local meteorological events, and (3) infrasonic emission from global meteorological events. The role of each of these contributions is discussed in turn.

Ambient pressure fluctuations.— The peripheral regions of a global meteorological event like gale, thunderstorm, tropical depression, or hurricane, are characteristically turbulent. At even modest levels of turbulence, ambient pressure fluctuations constitute the dominant signals detected by the microphones. This contribution is responsible for (1) the power law spectrum, which is characteristic of the equilibrium range of turbulence (ref. 8), and (2) the low coherence, because turbulent eddies, being much smaller than the microphone separation, are expected to be independent of each other at any two microphone sites. The slopes of the power spectra vary from about -0.5 to -3.5, depending upon the strength of the signal, and the mean coherence lies between 0.2 and 0.35. Furthermore these fluctuations create a strong background from which genuine infrasonic emissions must be extracted and are responsible for the low success rate in saving files on disk.

Infrasonic emissions from local meteorological events.— Since the classic paper of Lighthill (ref. 9) there has appeared a voluminous literature on aerodynamic sources of sound. In a particularly succinct treatment, Hardin (ref. 10), following an argument by Crow (ref. 11), points out that at low Mach numbers sound radiation is produced by "the action of vorticity within the flow," and that in a certain class of problems the sound source can be modelled as the interaction between a vortex and its image across the ground plane. A particularly fitting adaptation, for example, would be Caracena's vortex ring model of the microburst (ref. 12) together with Kambe and Minota's analysis of acoustic radiation from the head-on collision of two vortex rings (ref. 13). Unfortunately the spectral content of such radiation remains unknown, but the theoretical support for the microburst as a radiator of sound is encouraging. The sound spectrum will likely depend on the properties of the source, like its diameter, mean flow, and vorticity.

It is the contention here that the time delay estimates yielded by the adaptive filter algorithm converge only for the coherent contributions to the signal, i.e.

those generated by genuine infrasound propagating across the array, and that the filter extracts these signals from the much larger background due to the incoherent ambient turbulence. The locations depicted near the array in figure 11 are then presumed to represent local sources.

Infrasound emission from global meteorological events.— The ability of infrasound to propagate over vast distances is well documented. In fact, long-range infrasonic signals produced by Space Shuttle launches at Cape Canaveral, FL have been received on several occasions over a propagation distance of 660 miles at Langley Research Center. Theoretical support for the emission of infrasound by distant global events, associated with atmospheric turbulence, is given by Meecham (ref. 14), who specifies a f^{-2} power spectrum, and by Meecham and Ford (ref. 1), who predict a $f^{-7/2}$ spectrum for isotropic turbulence. Several of the files recorded in the present study yield hyperbolic loci with parallel asymptotes pointing in the direction of known storm centers, thus affording evidence for the existence of sources of this nature. As before, the spectra cannot be determined experimentally because of masking by ambient pressure fluctuations.

CASE HISTORIES

A list of the eleven global meteorological events, for which the concurrent class D activity was moderate-to-strong, is given in table 6. In addition, the number of class D files saved on disk and the mean slopes of the logarithmic auto power spectra are shown. Each of these events represents a case history, which will be discussed with the aid of a map containing a meteorological summary and a diagram showing the locations of experimentally determined infrasonic sources. A list of meteorological symbols used appears in table 7. A summary of local weather is given in table 8. Time is given as local time: Eastern Daylight Time prior to November 1 and Eastern Standard Time thereafter.

TABLE 6.- GLOBAL METEOROLOGICAL EVENTS CONCURRENT WITH MODERATE-TO-STRONG
INFRASONIC ACTIVITY

<u>Global Event</u>	<u>No. files</u>	<u>Mean slope</u>
1. Severe thunderstorm, PA-VA, 6/6/84	8	-1.13±0.86
2. Severe thunderstorm, KS-VA, 7/5/84	7	-1.88±0.87
3. Severe thunderstorm, WI-VA, 8/29-30/84	12	-1.00±0.75
4. Tropical Depression Arthur, 9/4/84	6	-1.15±0.65
5. Hurricane Diane, 9/12/84	10	-2.22±0.66
9/13/84	6	-0.82±1.06
6. Tropical Storm Isadore, 9/27/84	9	-1.49±1.07
7. Hurricane Josephine, 10/11-12/84	21	-1.35±1.10
8. Severe turbulence, eastern US, 11/2/84	9	-1.27±1.07
9. Gale, Great Lakes, 11/15/84	6	-1.06±0.80
10. Gales, western Atlantic, 11/20-24/84	12	-0.78±1.08
11. Gales and severe storms, eastern US, 12/5-6/84	8	-1.62±0.86

TABLE 7. METEOROLOGICAL SYMBOLS






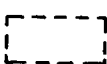



	Tropical storm (also used for gales)
	Hurricane
	Tornado
	Thunderstorm
	Severe turbulence
	Region affected by indicated event
	Region displaying lightening strikes on LLP
	Reference number assigned to event
	Array location
12/5 0600	Date and local time when event is reported
30-40 kt	Maximum windspeed of event in knots

TABLE 8.- LOCAL WEATHER DURING GLOBAL METEOROLOGICAL EVENTS

<u>Date</u>	<u>Temperature °F</u>	<u>Cloud cover</u>	<u>Windspeed, kt</u>		<u>Wind direction</u>	<u>Precipitation in.</u>
			<u>mean</u>	<u>gust</u>		
6/6/84	69-88	SCT-BKN	8-14	19	SW	0
7/5/84	75-91	SCT	12-18	29	S, SW	0
8/29/84	70-84	SCT-BKN	4-10	15	SW	0.01
8/30/84	73-90	SCT-BKN	6-12	18	SW	0
9/4/84	66-78	OVC	4-17	20	N	0.06
9/12/84	73-85	BKN-OVC	4-22	25	NE	0
9/13/84	73-82	BKN-OVC	3-13	18	E, SE	0.05
9/27/84	58-65	OVC	8-12	23	NE	T
10/11/84	63-72	BKN-OVC	1-12	17	N	0
10/12/84	62-73	BKN-OVC	6-14	20	N	0
11/2/84	55-74	BKN-OVC	7-17	25	N, NW	T
11/15/84	36-64	BKN	6-14	21	SW	0
11/20/84	33-40	CLR-SCT	6-14	24	NW	0
11/23/84	34-50	CLR-SCT	0-7	10	N	0
12/5/84	38-55	OVC	2-15	22	NE	0.69

Abbreviations: CLR - clear; SCT - scattered; BKN - broken; OVC - overcast;
T - trace.

1. Severe thunderstorm, Pennsylvania-Virginia, June 6, 1984

As a tornado swept across Minnesota and Wisconsin, a thunderstorm developed in central Pennsylvania in mid afternoon (fig. 20). The LLP's show an intense concentration of lightning strikes between Johnstown, PA and Hagerstown, MD from 1430 to 1618 hours. Later the strike region spread and descended southward to just north of Washington, DC.

In the time 1250-1940 hours eight class D signals were captured on the infrasonic array, whose source locations are shown in the insert. Three indicate source directions to the north, the direction of the storm, and five indicate local sources. The local weather showed no apparent effect of the storm, except for wind gusts up to 19 kt.

2. Severe thunderstorm, Kansas-Virginia, July 5, 1984

Severe thunderstorms were reported from Concordia, KS to Norfolk, VA between the hours 0200-0800. A moderate density of lightning strikes appeared simultaneously over West Virginia and over the southeastern corner of Pennsylvania between 1051 and 2015 hours (fig. 21). The local wind speed varied between 12-18 kt with gusts up to 29 kt.

Nine class D files were recorded between 1158 and 1448 hours, at which time the disk became full, because it contained seven files from the previous day. The number of attempts was 46, revealing an unusually high success rate of $9/46 = 19.6\%$. The insert shows that four files indicate signals from distant sources, in the direction of the lightning strikes, and three indicate local sources.

3. Severe thunderstorm, Wisconsin-Virginia, August 29-30, 1984.

A severe thunderstorm, with winds up to 70 kt, moved from Lone Rock, WI across Michigan to Utica, NY. A moderate concentration of lightning strikes appeared across central Pennsylvania and later descended to western Virginia (fig. 22). Local winds were moderate, gusting up to 15 kt on 8/29 and 18 kt on 8/30.

On 8/29 between 1535 and 1730 hours, six class D files were recorded out of 23 attempts, a 26.1% success rate. All but one indicated sources near the array (see insert). It is noteworthy that these occurred in the midst of the lightning activity in southwestern Virginia. On 8/30 the variance window of the filter was increased from 48 to 64 iterations, making it very difficult for a signal to pass the variance test. As a result the disk did not fill up until late 8/31. From 1242 hours on 8/30 until 2157 hours on 8/31 only six class D files were recorded out of 399 attempts, a 1.5% success rate. As shown in the insert, all the sources were located within the 5000 ft radius about the array.

4. Tropical Depression Arthur, September 4, 1984.

Starting NE of Puerto Rico, Tropical Depression Arthur moved northwesterly on 9/4 and 9/5, with modest winds up to 30 kt. Two simultaneous centers of lightning activity occurred south of Norfolk and in the Atlantic Ocean ENE of the array (fig. 23). Local winds were moderate, gusting up to 20 kt, and precipitation was light all day.

Six class D files were recorded between 1413 and 2328 hours, amidst the lightning activity. However, the first five of these occurred between 1413 and 1723 hours out of 36 attempts, a 13.9% success rate. The insert shows four sources close to the array and two pointing southward toward the lightning.

5. Hurricane Diane, September 12-13, 1984.

Hurricane Diane is especially significant to the present study for two reasons. First, it produced the strongest weather-related signals over the entire term of the study. Secondly, it remained stationary off the coast near Wilmington, NC for a full day and thus served as a source with known location. Its trajectory is shown in figure 24. Starting just north of the Bahamas on 9/8 with winds of 45 kt, it gathered strength as it paralleled the Florida coast and reached maximum intensity on 9/11, almost due east of Wilmington with winds of 135 kt. It hovered until the morning of 9/13, then moved inland with reduced winds of 80 kt, reversed its course across North Carolina, and dissipated at sea some time after 9/15. The period 9/12-9/13 was marked by a moderate concentration of lightning strikes in eastern North Carolina and west-central Pennsylvania. Starting in the late afternoon of 9/12 local wind speeds varied between 12-22 kt. Although the sky was continuously overcast, there was no precipitation. The wind speed persisted until the early afternoon of 9/13. The sky remained overcast, and 0.05 in. of rain fell by 1750 hours.

Between 1550 hours on 9/12 and 0815 hours on 9/13, corresponding to points 8 and 9 in figure 24, ten class D files were recorded out of 201 attempts, a 5% success rate. As shown in the insert, five files indicate far-field source directions ranging from 181° to 204° , while the actual bearing angle to the eye of the hurricane was 193° . The low success rate is surprising in view of the strength of the source, producing auto power spectral levels up to 85 dB, and its stationary location. The high levels of local wind are believed to have been a disrupting factor in preventing the TDE's from converging (see INTERPRETATION OF RESULTS).

The next two days, between 1349 hours on 9/13 and 1434 hours on 9/14, six of 153 attempts were recorded, a 3.9% success rate. During this period the fading hurricane moved across North Carolina back to sea. Five of the six recorded files indicated local sources (see insert). Again the gusty local wind may have disrupted the TDE convergence.

6. Tropical Storm Isadore, September 25-October 1, 1984.

Tropical Storm Isadore originated near San Salvador on 9/25, reached the Florida peninsula near West Palm Beach on 9/27, departed Florida near Jacksonville on 9/28, and dissipated at sea on 10/1. The trajectory is shown in figure 25. Its closest approach, about 200 miles from the array, occurred on 9/29 when it passed due east of Cape Hatteras. The storm was relatively weak, producing a maximum mean wind speed of 45 kt, and was not accompanied by lightning strikes, the LLP's being blank on both 9/27 and 9/28.

Between 1103 hours on 9/27 and 1501 hours on 10/1, corresponding to points 2 and 7 in figure 25, nine class D files were recorded out of 894 attempts, showing a 0.9% success rate. Six of the source locations were near the array and three indicated far-field sources toward the south, as shown in the insert. The local weather was mild, with winds from 8-12 kt and a trace of precipitation.

7. Hurricane Josephine, October 11-12, 1984.

Josephine became a hurricane 300 miles east of the Bahamas at 1330 hours on 10/9, moved northward to a position about 200 miles east of Norfolk at 2300 hours on 10/13, and then veered to the east (fig. 26). It reached its peak intensity of 100 kt at 0500 hours on 10/12, point 3, maintained 95 kt at point 4, and 75 kt at points 5 and 6. There were reports of severe turbulence north of Norfolk and in southern New England on 10/11 and 10/12 "due to outflow from Hurricane Josephine." The local skies were overcast and the weather surprisingly mild, with winds between 1-14 kt, gusting to 20 kt, and there was no precipitation.

In the time from 1149 hours on 10/11 to 0045 hours on 10/14 21 class D files were recorded, 7 on 10/11-12 and 14 on 10/12-14, out of 799 attempts for a 2.6% success rate. This time span corresponds to points 2-5 in figure 26. One insert shows nearly all source locations near the array, but the other shows two far-field sources from the east, possibly the hurricane itself or associated turbulence, and two from the south, which have no apparent meteorological association.

8. Severe turbulence, eastern United States, November 2, 1984.

Throughout 11/2 the National Weather Service reported severe turbulence at two locations, across Illinois and across the entire northeastern US, as shown in figure 27. The conditions in the northeast were "reported by several large aircraft" and were "due to strong low level winds with possible low level wind shear." The turbulence moved slowly eastward throughout the day. The LLP showed only two lightning strikes, both in the Atlantic Ocean southeast of Norfolk. There was no indication of a storm occurring anywhere along the entire eastern US. The local weather featured broken to overcast cloud cover, winds from 7-17 kt gusting to 25 kt, and a trace of precipitation.

From 1416 hours on 11/2 until 1456 hours on 11/3 five class D files out of 313 attempts were saved on disk for a 1.6% success rate. The disk did not become full until 1316 hours on 11/5. Altogether nine class D files were saved over the three-day period (see insert, fig. 27). The infrasonic signals were just about as intense as any received during the hurricanes and thunderstorms. This is the only one of the eleven case histories not associated with a global meteorological event.

9. Gale, Great Lakes, November 15-19, 1984.

A gale, starting north of Lake Superior at 0600 hours on 11/15 (point 1 in fig. 28), moved eastward and reached point 2 at 0600 hours on 11/16, with winds from 25-40 kt. From 11/16-11/17 the National Weather Service reported severe turbulence below 8000 ft in the northeast (region 3) "due to low level winds with low level wind shear possible within 2000 ft above ground level." In the midwest (region 4) turbulence was reported on 11/9 at altitudes from 20-28 000 ft. The LLP's showed only four lightning strikes on 11/16, all in the Atlantic Ocean, and none thereafter through 11/19. Locally the winds varied between 6-14 kt with gusts up to 21 kt, the cloud cover was broken, and there was no precipitation.

On 11/15 and 11/16 six class D files were saved. However, five of these occurred in relatively rapid succession, from 1315 to 2115 hours on 11/16. Most indicated locations close to the array (see insert, fig. 28). Since there were 96 attempts over this six hour period, the success rate was an unusually high 5.2%. The intensity of the infrasonic signals was modest when compared to those of the previous severe storms.

10. Gales, western Atlantic, November 20-24, 1984.

Two gales developed in the Bahamas during this time interval (fig. 29). The first started at 0000 hours on 11/22, moved eastward, veered northward to the closest approach to the array (point 3) at 0600 hours on 11/23, then resumed an eastward course. The second started at 1200 hours on 11/23 and moved on a generally eastward course until 11/25. Wind speed varied from 25-45 kt for both gales. The LLP system was shut down for maintenance.

Meanwhile the National Weather Service reported two regions of severe turbulence. One region, covering most of the states of Georgia, South Carolina, and North Carolina, was "reported by several aircraft" between 2000-2400 hours on 11/21 and was said to be "due to wind shear associated with the jet stream." The other region, covering the Florida peninsula, was reported by "several aircraft in this area" between 1335 hours on 11/22 and 0345 on 11/24. This low level turbulence was "due to northeasterly winds." The local weather report showed scattered to clear cloud cover, winds from 0-14 kt, and no precipitation from 11/20-11/24.

In the time from 1824 hours on 11/20 to 1819 hours on 11/22 eight class D files were recorded out of 575 attempts for a 1.4% success rate. However, five of these files clustered within 145 attempts, from 0614-1819 hours on 11/22 for a 3.4% success rate. This cluster coincided with the gale movement from points 1 to 2 and with the Florida turbulence 10. Five of the eight files (see insert, fig. 29) indicate a source direction toward the south, the location of the turbulence; but in order to generate infrasonic signals that are detectable after propagating some 600 miles, the turbulence would have had to be very severe.

A second disk contained four class D files from 1306 hours on 11/23 to 1536 hours on 11/24. These required 318 attempts for a 1.3% success rate. During this time the gale moved from point 2 to 3 and the Florida turbulence was still active. Two of the files (see insert, fig. 29) indicate southerly source directions. However, most of the locations shown in both inserts indicate local sources.

11. Gales and severe storms, eastern United States, December 5-6, 1984.

The period 12/5-6/84 was marked by widespread meteorological activity (fig. 30). A gale, developing in the Gulf of Mexico early on 12/5, swept inland across the southeast and reached New England at midday on 12/6. Wind speeds were in the range 25-60 kt. Thunderstorms broke out along its path, including one at Norfolk at 0000 hours on 12/6. The LLP revealed a moderate density of lightning strikes in the Atlantic Ocean southwest of Norfolk between 1109-1900 hours on 12/6. The National Weather Service reported three regions of severe turbulence. In a region extending from Ohio to New Jersey "severe turbulence . . . due to jet stream wind shear [was] reported by several aircraft" from 12/5-6. In a second region covering Arkansas and half of Mississippi and Alabama, "severe turbulence . . . due to wind shear in the vicinity of the upper jet stream" was reported on 12/6. Finally there were "several aircraft reports of severe turbulence" over New England "due to wind shear" on 12/6. The local weather showed overcast skies, winds from 2-15 kt gusting to 22 kt, and 0.69 in. of precipitation.

From 1830 hours on 12/5 until 1120 hours on 12/7 eight class D files out of 490 attempts were saved on disk, for a success rate of 2.1%. This period coincides with the storm on the trajectory from points 3-6 in figure 30, with the lightning strikes, and with the severe turbulence in all regions. Two files indicate source directions toward the lightning strikes but most are clustered near the array

(see insert). Again the infrasonic signal amplitudes were moderate when compared to those of the prior severe storms.

INTERPRETATION OF RESULTS

The decisive issue of this study is whether or not the class D signals, received at the microphone array, originate from meteorological sources. Two facts point in favor of an affirmative answer, and two against. First, in favor, moderate-to-strong class D activity appeared concurrently with significant meteorological events (SIGMETS). Conversely, in the absence of SIGMETS, signatures of other classes prevailed, most of these identifiable with man made events. Secondly, despite the low coherence associated with class D signatures, the time delay estimates yielded source locations with precise definition, as is evident in figures 7 and 8 -- these are typical of the data. On the negative side, in times of intense meteorological activity there were unexpectedly long lapses between files saved on disk. In other words, the success rate was low. In the case of Hurricane Diane, for example, a known source remained stationary for a full day; yet the average interval between successful saves was 20 attempts. Secondly, the infrasonic signature of a local source, like a microburst, has no theoretical guidelines, a fact which makes consistent source recognition all the more difficult.

The problem of locating a source, in the midst of "diffuse noise," on a two-element array has been treated by Bendat and Piersol (ref. 15). Their analysis not only sheds some light on the matter but allows a plausible explanation for the lack of continuity in the acceptance of infrasonic signatures. The coherence function and phase angle of the signals at microphones A and B in figure 2 are given by the following equations:

$$\gamma_{AB}^2(f) = [1 + R(f)]^{-2} \left\{ \left[R(f) \frac{\sin kd}{kd} + \cos k_t d \right]^2 + \sin^2 k_t d \right\} \quad (7)$$

$$\phi_{AB}(f) = \tan^{-1} \left[\frac{\sin k_t d}{R(f) (\sin kd)/kd + \cos k_t d} \right], \quad (8)$$

in which

$$R(f) = G_d(f)/G_s(f) \quad (9)$$

$$k = 2\pi f/c \quad (10)$$

$$k_t = (2\pi f/c) \cos \theta \quad (11)$$

and $G_d(f)$ and $G_s(f)$ are the autospectra of the diffuse noise and coherent source respectively. The standard deviation of the phase estimate due to statistical sampling considerations depends strongly upon the coherence function:

$$\sigma(\phi_{AB}) \approx \sin^{-1} \left[\frac{1 - \gamma_{AB}^2(f)}{2n_d \gamma_{AB}^2(f)} \right]^{1/2} \quad (12)$$

where n_d is the number of data blocks which are averaged to obtain the estimates. For the class D signatures evaluated here $\gamma_{AB}^2(f) \approx 0.25$, $n_d = 2$, hence $\sigma(\phi_{AB}) \approx 60^\circ$. As is pointed out in reference 15, the presence of $R(f)$ in the denominator of equation (8) causes $\phi_{AB}(f)$ to deviate from the familiar linear dependence upon frequency; rather $\phi_{AB}(f)$ undulates about a straight line and is accurate only at frequencies where

$$k_t d = n\pi, n = 1, 2, \dots \quad (13)$$

From equation (11) the frequencies for which equation (13) is fulfilled are

$$f_n = nc/(2d \cos \theta) \quad (14)$$

The next task is to relate the standard deviation $\sigma(\theta)$ of the angle of incidence to that of the phase angle $\sigma(\phi_{AB})$. Starting from

$$\phi_{AB} = 2\pi fd \cos \theta/c \quad (15)$$

one finds

$$\sigma(\theta) = c\sigma(\phi_{AB})/2\pi fd \sin \theta \quad (16)$$

and upon inserting (14) for the optimal frequency ($n = 1$) obtains

$$\sigma(\theta) = \sigma(\phi_{AB})/\pi \tan \theta \quad (17)$$

It appears that $\sigma(\theta)$ will be extremely large at small angles of incidence and extremely small at angles near normal incidence, but in reality both cases have limitations due to the finite bearing resolution. Table 9 shows $\sigma(\theta)$ for angles corresponding to an uncertainty of one bearing resolution at parallel ($\theta = 0^\circ$) and normal ($\theta = 90^\circ$) incidence, as well as for an intermediate angle ($\theta = 45^\circ$).

TABLE 9.- RESOLUTION AND STANDARD DEVIATION OF BEARING ANGLE

<u>Incidence</u>	<u>$\Delta\theta$</u>	<u>θ</u>	<u>$\sigma(\theta)$</u>
Parallel	13.2°	13.2°	81.7°
Intermediate	2.1°	45°	19.2°
Normal	1.5°	88.5°	0.51°

Examination of table 9 reveals the reason for the poor success rate for saving files on disk, even amidst intense meteorological activity. According to equation (4) the TDE routine will accept files only if the time delays are consistent to within ± 3 digital increments, corresponding to ± 3 bearing resolutions or one bearing resolution per microphone pair. If the error is random, then the probability P that a measured bearing angle will fall within the acceptance interval $\pm \Delta\theta'$ about the mean is given by the Gaussian distribution:

$$P = [2\pi \sigma^2(\theta)]^{-1/2} \int_{-\Delta\theta'}^{\Delta\theta'} \exp [-x^2/2\sigma^2(\theta)] dx \quad (18)$$

If infrasound is produced continuously by class D meteorological events, then the success rate is equal to the acceptance probability P ; otherwise the success rate is P times some intermittency factor. For parallel, intermediate, and normal incidence, equation (18) together with the data of table 9 yields acceptance probabilities of 12.9%, 8.5%, and 99.7% respectively. If the infrasonic source lies outside the array, then in general two of the three angles of incidence will lie in the "intermediate incidence" category, in which case the acceptance probability is expected to be about 8.5%.

In the case of Hurricane Diane, a strong source, the success rate on 9/12/84 was 5.0%, in good agreement with the computed acceptance probability of 8.5%. It is thus concluded that the hurricane, as it hovered near Wilmington, NC for a full day, emitted infrasound and induced local sources almost continuously. Global events having a success rate of 2%, on the other hand, accordingly had an intermittency factor on the order of $(2/8.5) \times 100 = 24\%$; in other words, infrasound-producing events occurred only 24% of the time. The results for both cases is reasonable.

Surprisingly it does not require much diffuse noise to produce a low coherence. Equation (7) reveals that the coherence $\gamma_{AB}^2(f)$ will be about 0.25 when the signal-to-noise power is 1:1. The diffuse noise power spectrum is known from plots such as shown in figure 19 and fits an expression of the form

$$G_d(f) = A_o f^{-A_1} \quad (19)$$

where typical values are $A_o = 10^5$ and $A_1 = 1.8$. Since $\gamma_{AB}^2(f)$ is found to be nearly frequency-independent, it follows from equation (19) that the form of $G_s(f)$ cannot differ too much from equation (19). Let

$$G_s(f) = B_o f^{-B_1} \quad (20)$$

If $|A_1| > |B_1|$ then $\gamma_{AB}^2(f)$ will increase with frequency. If $|A_1| < |B_1|$ it will decrease with frequency. Experimentally both cases have been observed. Furthermore, for the numerical values of the parameters pertinent to the present

array, $\gamma_{AB}^2(f)$ shows very little dependence upon the angle of incidence. Figure 31 shows a plot of equation (7) with $A_0 = 10^5$, $A_1 = 2.5$ (see top of fig. 13), $B_0 = 5 \times 10^4$, $B_1 = 2.0$, $\theta = 60^\circ$. Agreement with the top curve of figure 14, from 2-16 Hz, is quite good. Thus the flat coherence function indicates that the spectral shape of the infrasonic source must nearly follow that of the diffuse noise.

A PRACTICAL PASSIVE INFRASONIC WIND SHEAR ALERT SYSTEM

A practical system must be designed to achieve the following operating conditions: (1) maximum success rate for accepting pertinent signatures; (2) minimum lag time between sensing and indicating an event; (3) maximum accuracy in locating a source. Unfortunately these have conflicting requirements on signal processing parameters. Obviously a success rate significantly greater than the present 5% will be required in a practical system. This can be improved by expanding the acceptance angle $\Delta\theta'$, at the expense of accuracy in source location, and by reducing the standard deviation $\sigma(\theta)$, a step which will require more block averages at the expense of frequency resolution. The following step-by-step procedure delineates the requisite design compromises.

(1) Let the bandwidth extend from 2 to 20 Hz. Lower frequencies are dominated by the wind; and higher frequencies, extending into the audio range, can suffer interference from man-made sources, especially in the vicinity of an airport. Further, let the frequency resolution be $\Delta f = 1$ Hz; then the sample period will be $T = 1/\Delta f = 1$ sec, and 19 components will be available for source identification. This number should be sufficient.

(2) Let the sample number per block be $N = 128$. Then the sample interval will be $\Delta t = T/N = 1/128$ sec and the sample rate $f_s = 128$ Hz, which is $128/20 = 6.4$ times the filter frequency and should be very effective in suppressing aliasing.

(3) Let the sample time window be $T_d = 10$ sec. Then the number of block averages will be $n_d = T_d/T = 10/1 = 10$. This will reduce the standard deviation $\sigma(\theta)$. If the computational time is 5 sec, then the total lag time will be $10 + 5 = 15$ sec, which should be acceptable.

(4) According to equation (2a) the bearing resolution will be 0.85° at an incident angle $\theta = 45^\circ$. This is much too sharp to allow a high success rate. Rather let the acceptance angle $\Delta\theta'$ be five bearing resolutions, i.e. $\Delta\theta' = 5 \Delta\theta = 4.3^\circ$. The source location error at a range of 5000 ft will then be $\Delta R = R\Delta\theta' = 5000 \times 4.3^\circ \times \pi/180^\circ = 375$ ft, which is still reasonable. Note that the acceptance angle can be widened by reducing the array spacing d . This will be discussed below.

(5) According to equations (12) and (17) the standard deviation of the incident angle is $\sigma(\theta) = 7.25^\circ$ at $\theta = 45^\circ$. This together with $\Delta\theta' = 4.3^\circ$ leads to an acceptance probability $P = 44.4\%$ [eq. (18)]. In other words, an emitting event will be detected by a single array about half the time.

The acceptance probability can be improved by further widening the frequency resolution Δf , but fewer components would be available to identify the source; or by increasing the acceptance angle $\Delta\theta'$, but the source location would become more uncertain.

Further improvements may be realized through reducing the array spacing and adding more elements to the array. The array spacing can be reduced to $d = 160$ ft, while retaining a bearing resolution (and acceptance angle) of $\Delta\theta = \Delta\theta' = 4.3^\circ$. A reduction in d may in addition improve the coherence of the infrasonic signal, but, depending on eddy size, it may also lead to coherence in turbulent pressure fluctuations at the three microphone sites. Further testing is required to resolve this question. Additional elements in the array will require modification of the signal processing algorithm and more powerful computational capability.

A summary of proposed modifications in signal processing parameters are listed alongside the original parameters in table 5.

ACKNOWLEDGMENT

Part of this work was performed by J. W. Stoughton and C. S. Khalaf, Old Dominion University, under NASA contract NAS1-17099-33.

NOTE

The National Aeronautics and Space Administration does not endorse commercial products. Products of other manufacturers comparable to those specified in this memorandum would have probably performed as well.

REFERENCES

1. Meecham, W. C.; and Ford, G. W.: "Acoustic Radiation from Isotropic Turbulence," J. Acoust. Soc. Am., Vol. 30, No. 4, April 1958, pp. 318-322.
2. McDonald, John A.: "Naturally Occurring Atmospheric Acoustical Signals," J. Acoust. Soc. Am., Vol. 56, No. 2, August 1974, pp. 338-351.
3. Bowman, H. S.: "Frequency Spectra Information on Storm-Related Infrasound," J. Acoust. Soc. Am., Vol. 55, No. 5, May 1974, pp. 927-928.
4. Georges T. M.: "Infrasound from Convective Storms: Examining the Evidence," Rev. Geophys. Sp. Phys., Vol. 11, No. 3, August 1973, pp. 571-594.
5. Bedard, A. J.: "Infrasound Originating Near Mountainous Regions in Colorado," J. Appl. Meteor., Vol. 17, No. 7, July 1978, pp. 1014-1022.
6. Posmentier, E. S.: "1-16-Hz Infrasound Associated with Clear Air Turbulence Predictors," J. Geophys. Res., Vol. 79, No. 12, April 20, 1974, pp. 1755-1760.
7. Khalaf, Camille S.; and Stoughton, John W.: "Design of Infrasound-Detection System via Adaptive LMSTDE Algorithm," Final Report NASA Research Contract 1-17099 No. 33, Old Dominion University, November 1984.
8. Hinze, J. O.: Turbulence, An Introduction to its Mechanism and Theory, McGraw-Hill Book Company, 1959, Ch. 3.
9. Lighthill, M. J.: "On Sound Generated Aerodynamically II. Turbulence as a Source of Sound," Proc. Roy. Soc. A, Vol. 222, 1954, pp. 1-32.
10. Hardin, J. C.: "Noise Calculation on the Basis of Vortex Flow Models," ASME Symposium on Noise and Fluids Engineering, Atlanta GA, November 28-30, 1977.
11. Crow, S. C.: "Aerodynamic Sound as a Singular Perturbation Problem," Stud. App. Math., Vol. 49, No. 1, March 1970, pp. 21-44.
12. Campbell, C. Warren: "A Spatial Model of Wind Shear and Turbulence for Flight Simulation," NASA Technical Paper 2313, May 1984.
13. Kambe, T.; and Minota, T.: "Acoustic Wave Radiated by Head-On Collision of Two Vortex Rings," Proc. Roy. Soc. Lond., Vol. A386, 1983, pp. 277-308.
14. Meecham, W. C.: "On Aerodynamic Infrasound," J. Atmos. Terres. Phys., Vol. 33, 1971, pp. 149-155.
15. Bendat, Julius S.; and Piersol, Allan G.: Engineering Applications of Correlation and Spectral Analysis, John Wiley and Sons, 1980, Ch. 3.

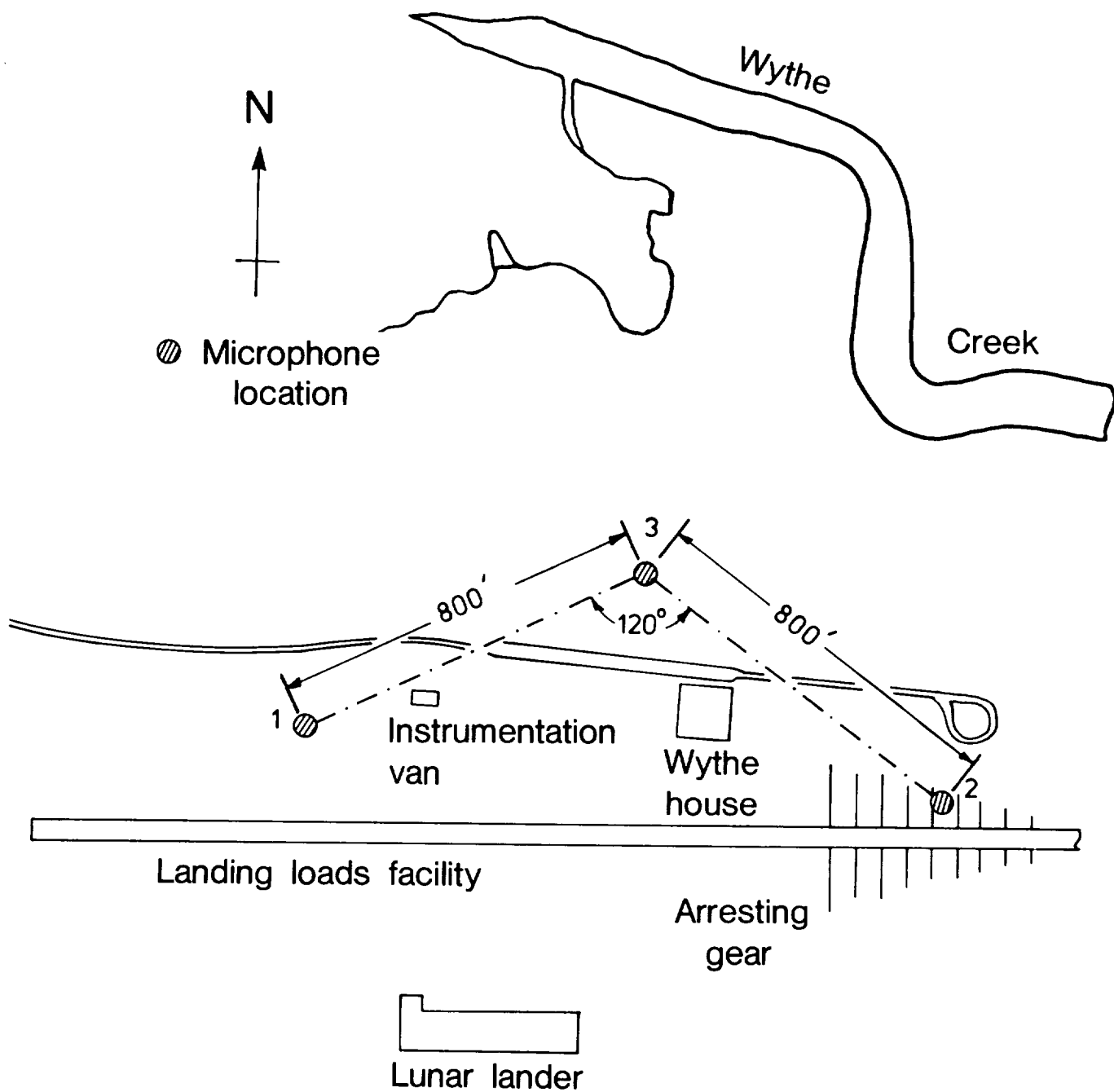


Figure 1.- Layout of the array.

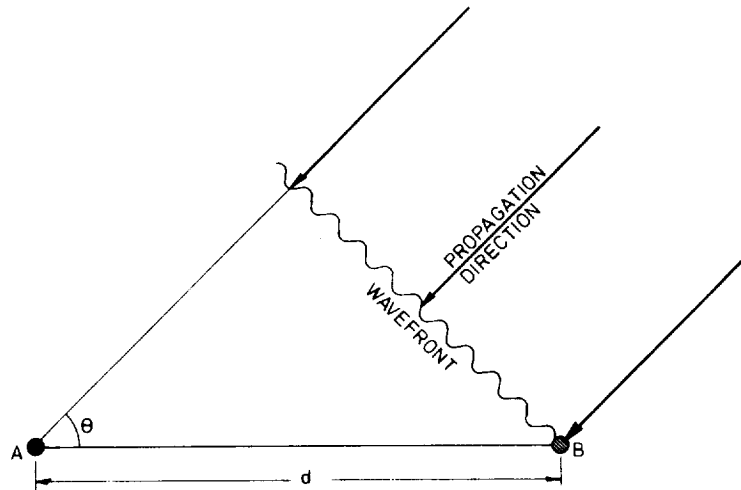


Figure 2.- Infrasonic wave incident upon a microphone pair.

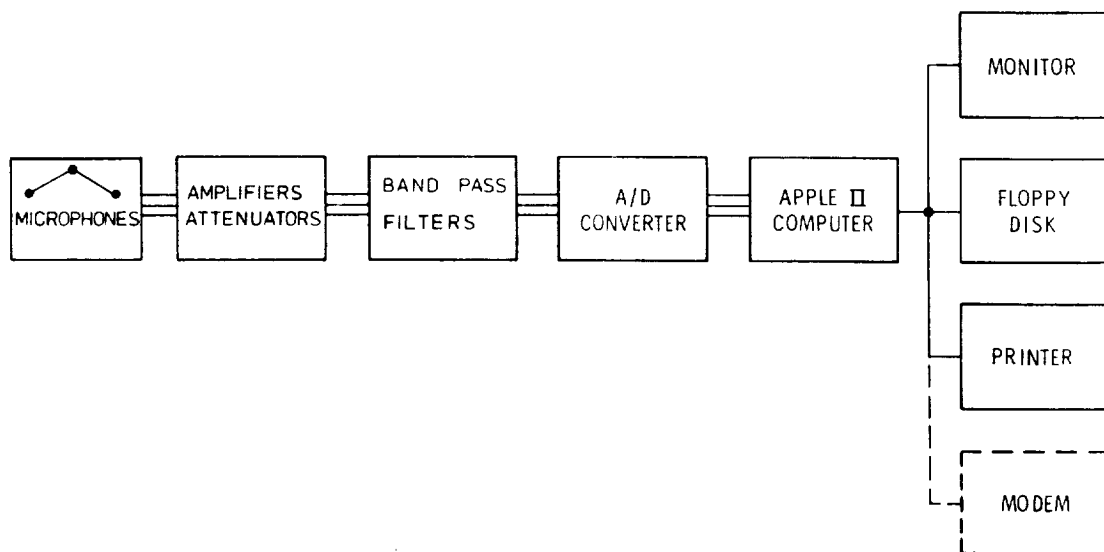


Figure 3.- Block diagram of the instrumentation.

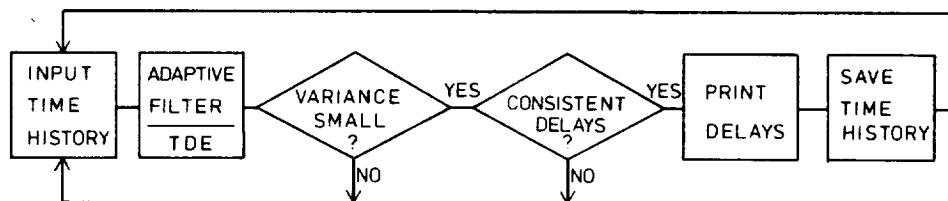


Figure 4.- Time delay estimation (TDE) routine.

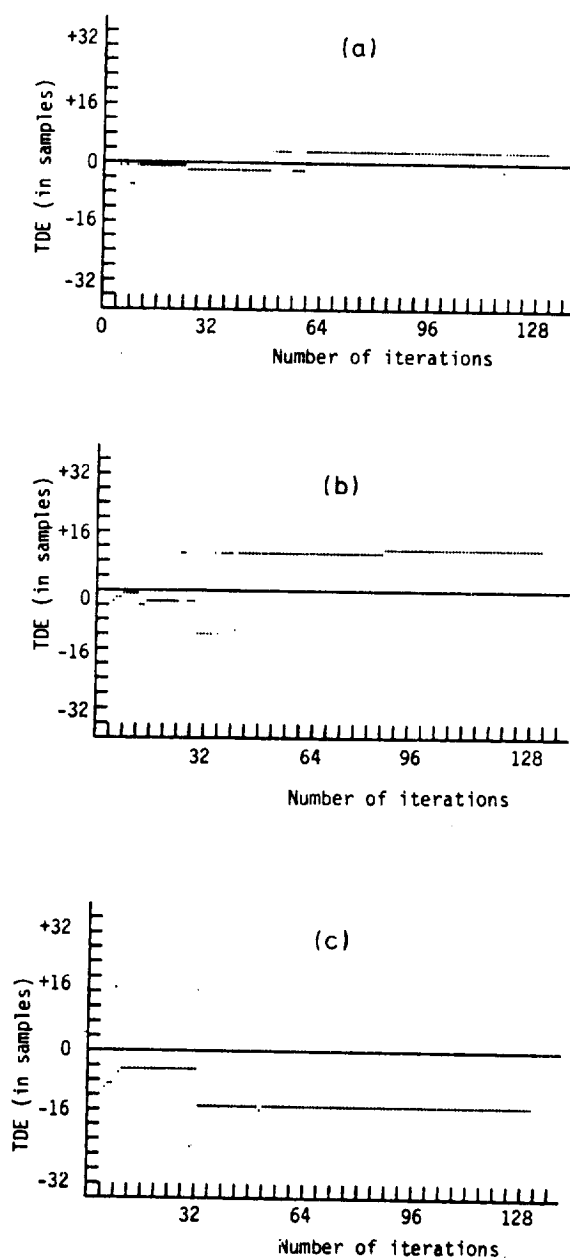


Figure 5.- Time delay estimate versus number of iterations for three microphone pairs: (a) C1 x C2, (b) C2 x C3, (c) C3 x C1. Each TDE sample on the ordinate corresponds to 0.039 sec. Thus C1 leads C2 by $3 \times 0.039 = 0.1172$ sec; C2 leads C3 by $11 \times 0.039 = 0.4296$ sec; and C3 lags C1 by $14 \times 0.039 = -0.5468$ sec.

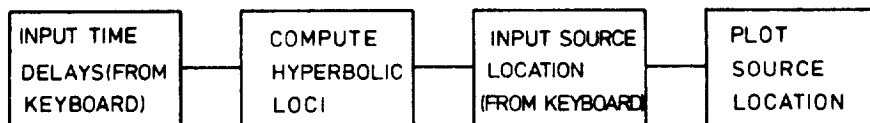


Figure 6.- Source location routine.

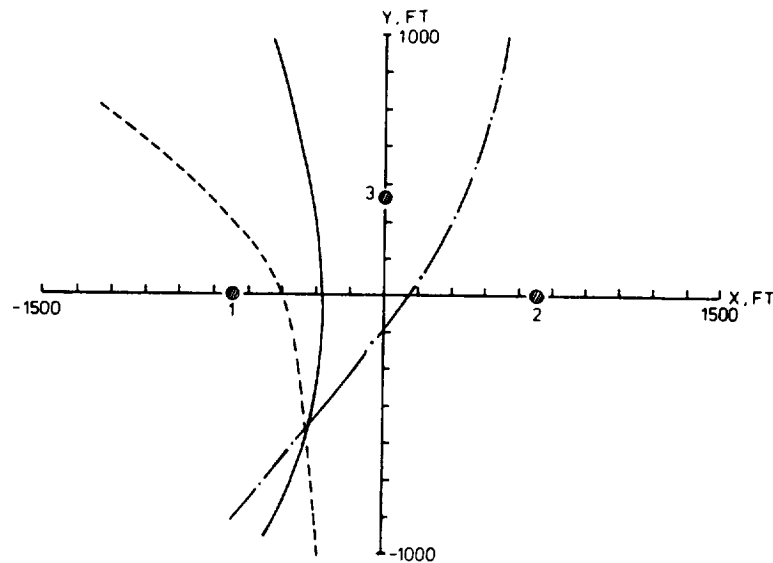


Figure 7.- Source location hyperbolas for a local source. The shaded circles are microphones. The hyperbolas represent possible locations of a source producing a signal at microphone pairs C1 x C2 (solid line), C2 x C3 (dot-dashed line), and C3 x C1 (dashed line). The respective time delays are 0.4687, -0.1562, and -0.3125 sec between microphone pairs. The intersection of the three hyperbolas locates the source at (-335, -490) ft.

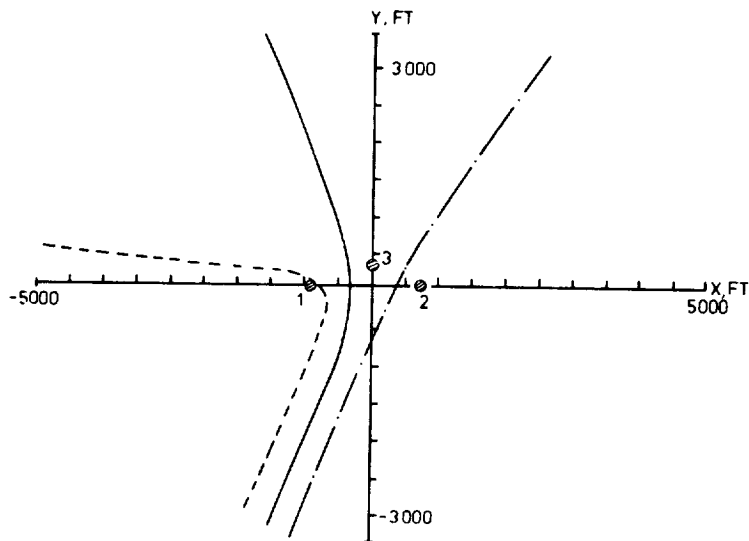


Figure 8.- Source location hyperbolas for a distant source. The shaded circles are microphones. The hyperbolas represent possible locations of a source producing a signal at microphone pairs C1 x C2 (solid line), C2 x C3 (dot-dashed line), and C3 x C1 (dashed line). The respective time delays are 0.5163, 0.0866, and -0.5859 sec. The asymptotes of the three hyperbolas indicate a source direction of 205° with respect to the y-axis.

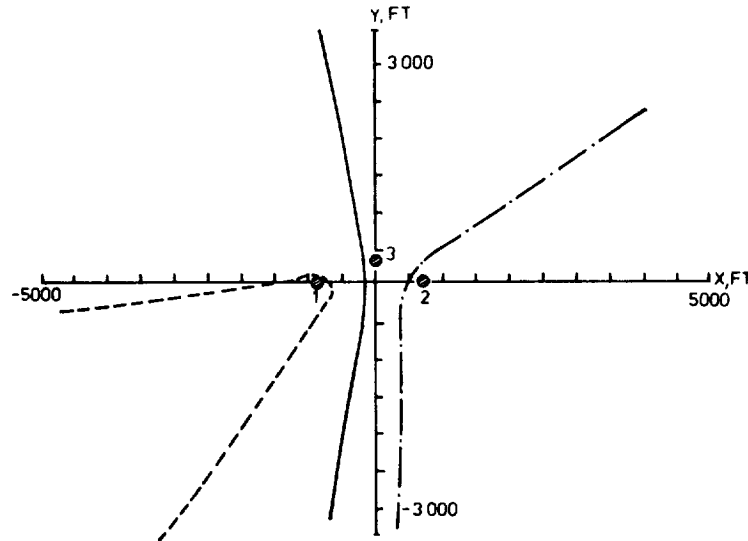


Figure 9.- Source location hyperbolas for a distant source at a large elevation. The shaded circles are microphones. The hyperbolas represent possible locations, projected on the ground, of a source producing a signal at microphone pairs C1 x C2 (solid line), C2 x C3 (dot-dashed line), and C3 x C1 (dashed line). The respective time delays are 0.2734, 0.3515, and -0.6579 sec. The nonparallel asymptotes prevent determination of the source direction.

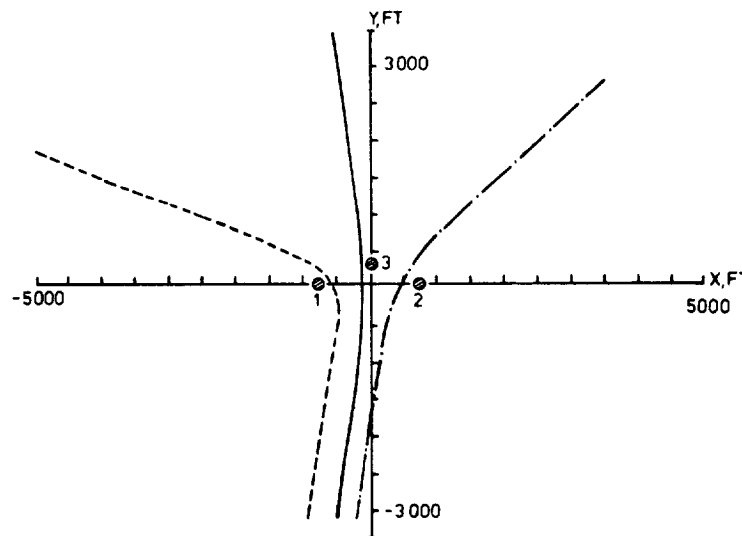


Figure 10.- The same hyperbolas as in figure 9 corrected for source elevation [eq. (5)]. The time delays are multiplied by 0.707, corresponding to an elevation angle of 45° . Now the asymptotes are parallel, indicating a source direction of 190° with respect to the y-axis.

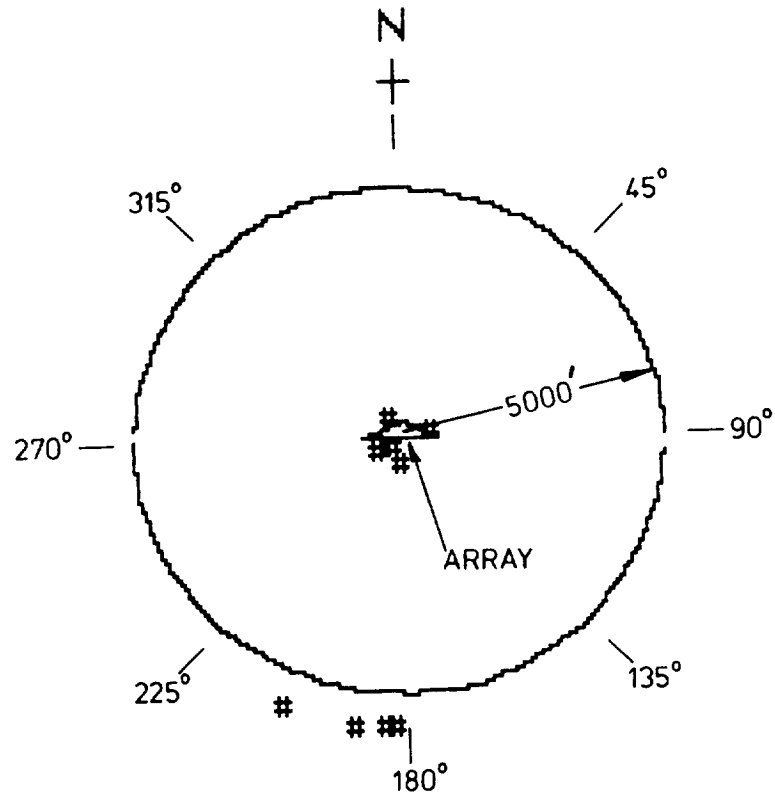


Figure 11.- Source location map. The triangle in the center is the microphone array. The cross-hatches are source locations, as determined from the TDE's. Beyond the 5000 ft radius the system resolution does not permit local and distant sources to be distinguished.

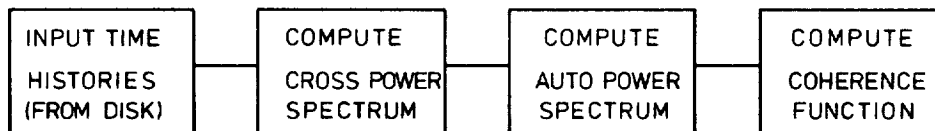


Figure 12.- Source identification routine.

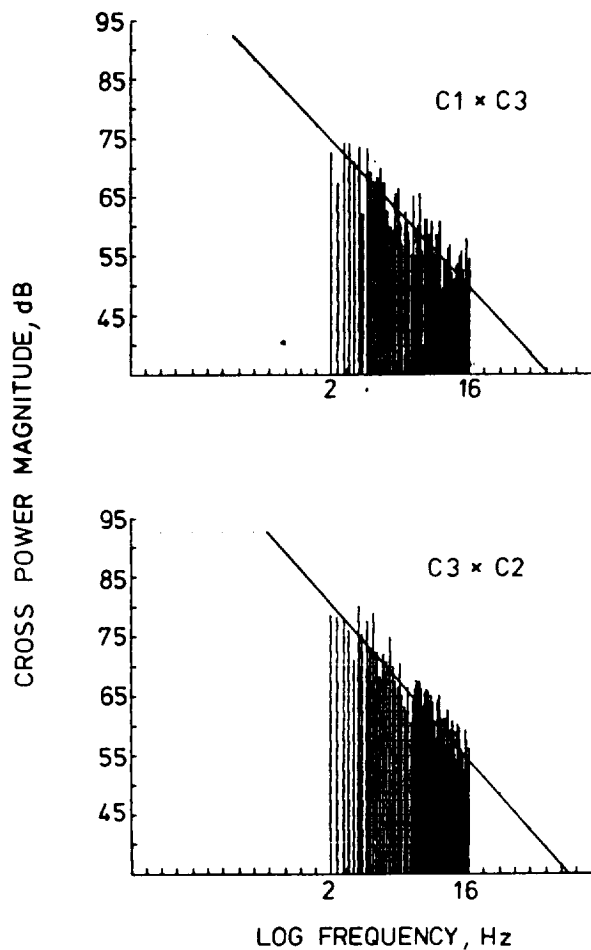


Figure 13.- Cross power magnitude spectrum for two microphone pairs. The straight line represents the best linear fit.

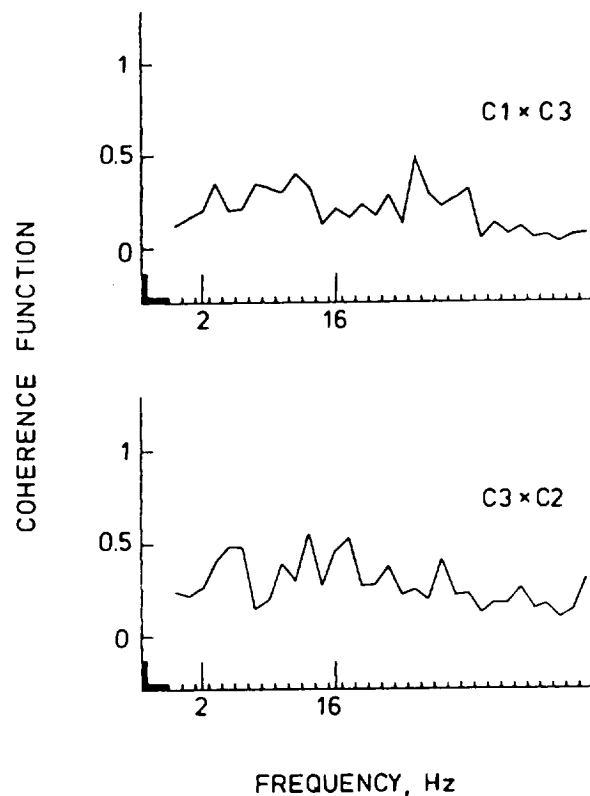


Figure 14.- Coherence function for the data shown in Figure 13. The linear plot facilitates identification of highly coherent frequency components. The mean values of coherence from 2-12.8 Hz are 0.242 and 0.350 respectively.

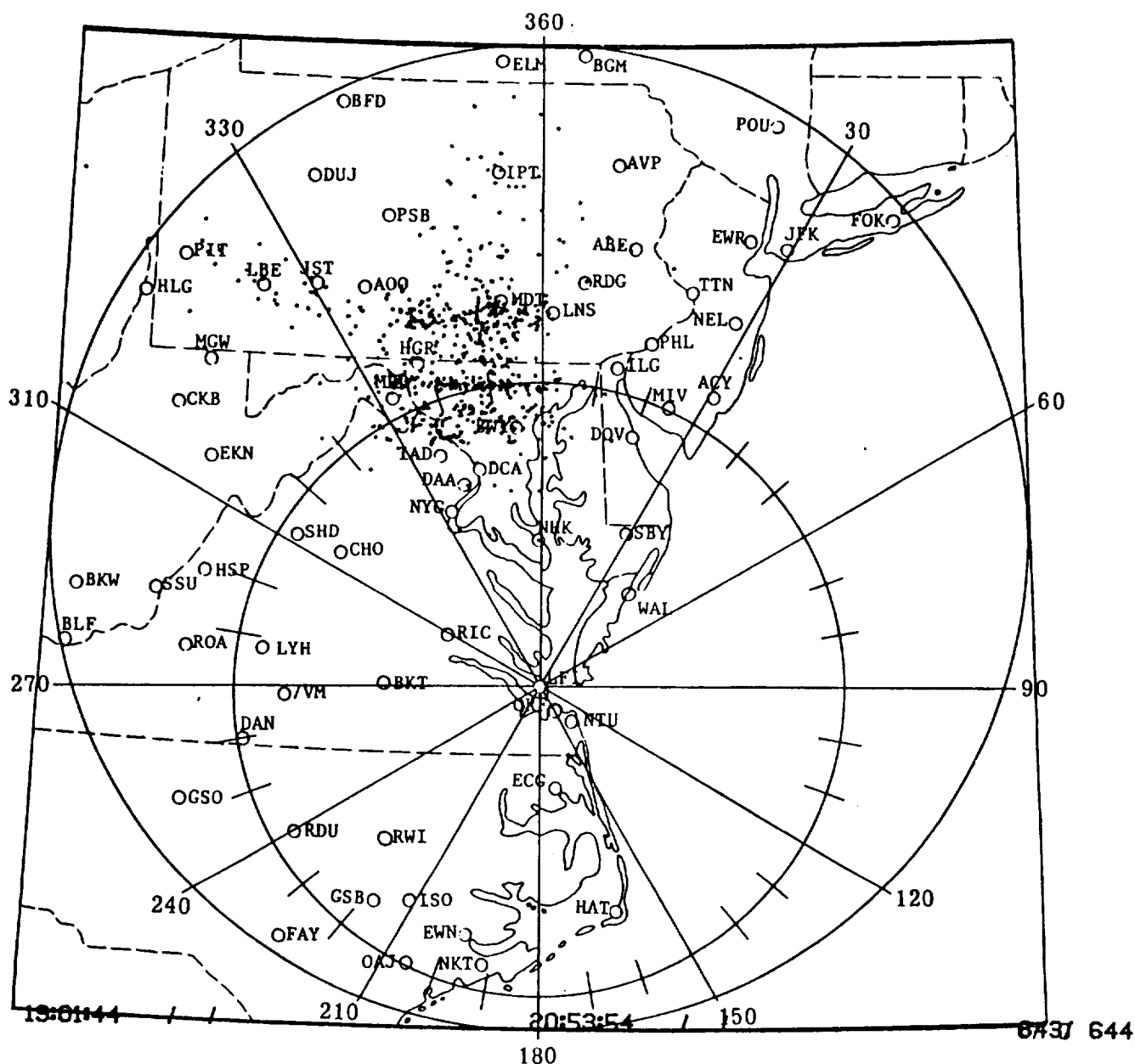


Figure 15.- Lightning locator plot (LLP) recorded on June 6, 1984 between the hours 1901 and 2053 local time. Each dot represents a cloud-to-ground strike. National Weather Service stations are designated by three-letter codes, e.g. RIC = Richmond. The coordinates are centered at Langley Field.

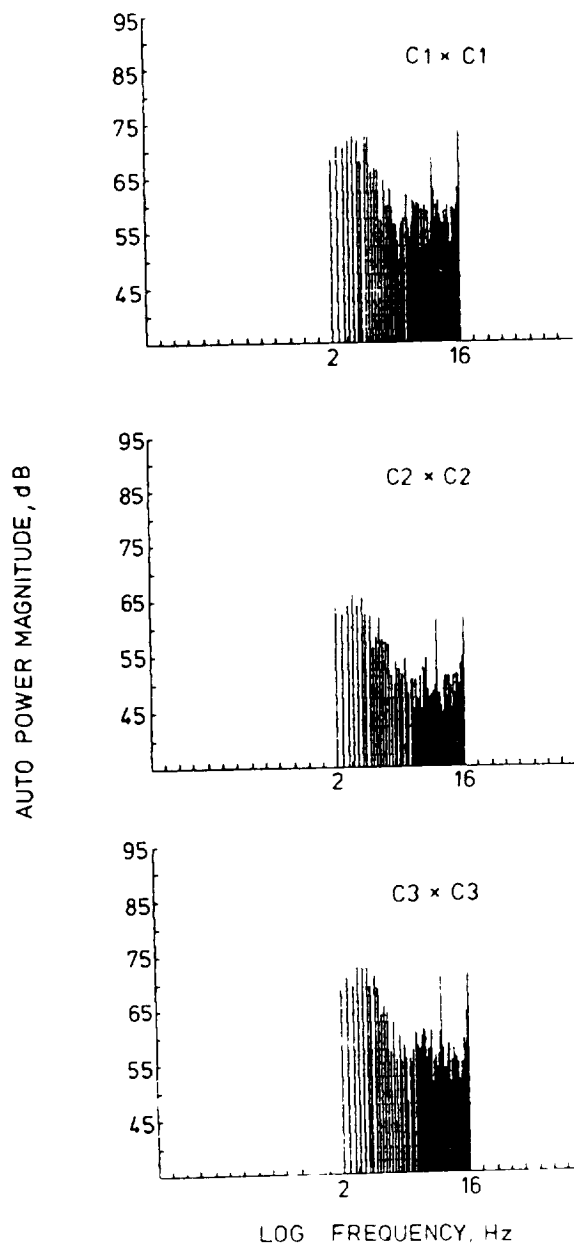


Figure 16.- Class A infrasonic signature. The auto power spectra for all three microphone pairs reveal a peak at a frequency of about 3 Hz. This is believed to be the spectrum of a sonic boom from a jet aircraft maneuvering in the vicinity of the array.

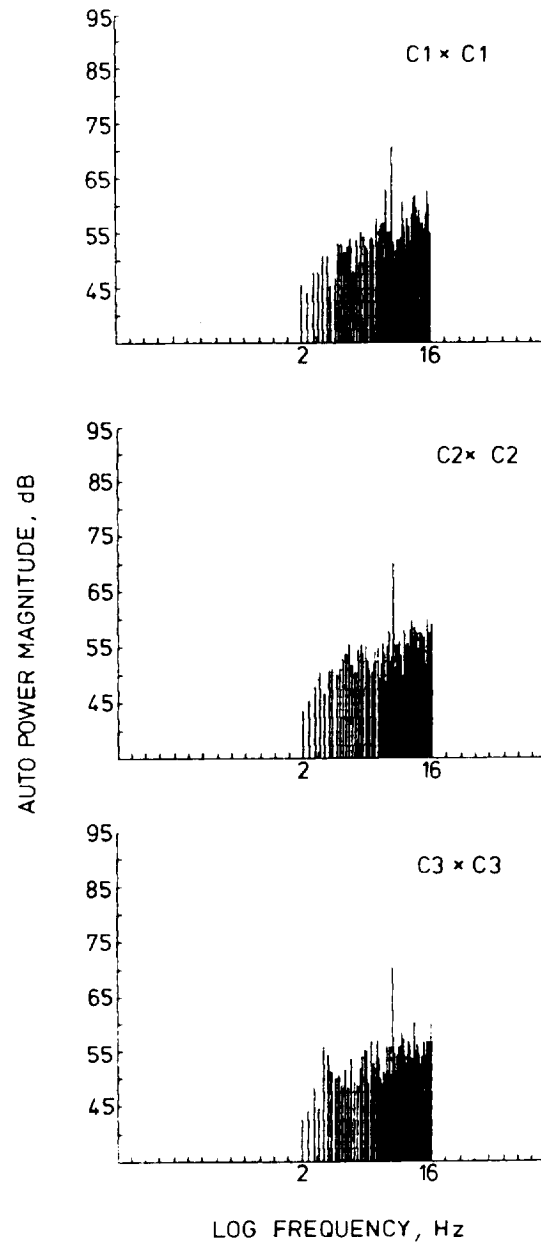


Figure 17.- Class B infrasonic signature. The pronounced discrete frequency at 8 Hz in all three auto power spectra is believed to dominate the TDE.

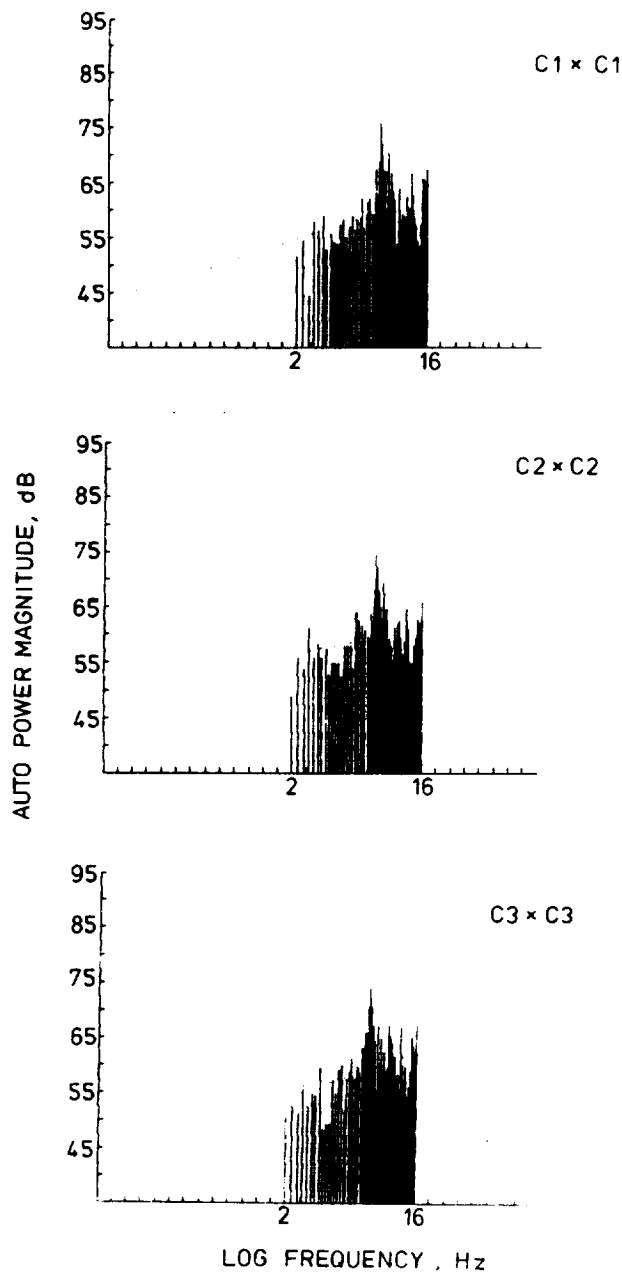


Figure 18.- Class C infrasonic signature. This is similar to the Class B signature, except that the peak, centered here at 5.6 Hz, has a bandwidth of a few discrete components.

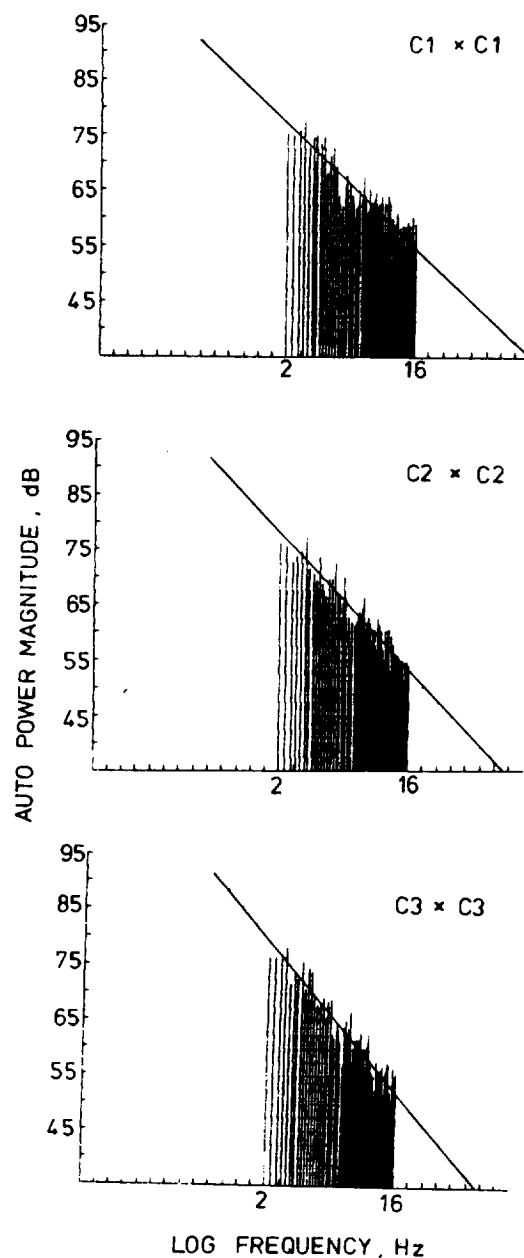


Figure 19.- Class D infrasonic signature. The auto power spectra reveal a good fit to a straight line, as shown in the figure. The best-fitted slopes are -2.50, -2.78, and -3.05 for microphones C1, C2, and C3. The correlation coefficients for the best fit are -0.911, -0.943, and -0.943. The auto power spectra are computed from the same data as shown in Figure 13.

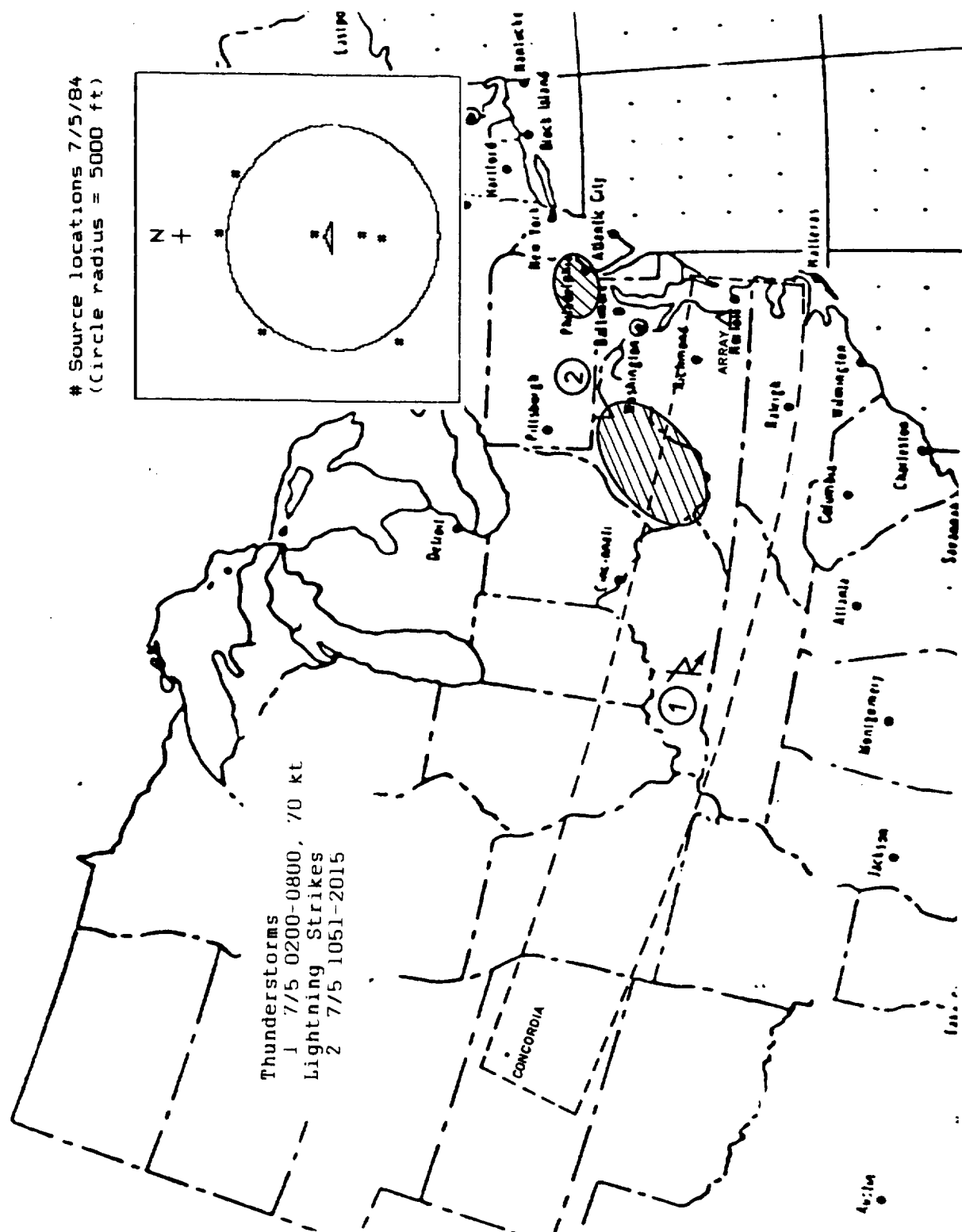


Figure 21.- Meteorological events and source locations (insert) of July 5, 1984.

ORIGINAL PAGE IS
OF POOR QUALITY

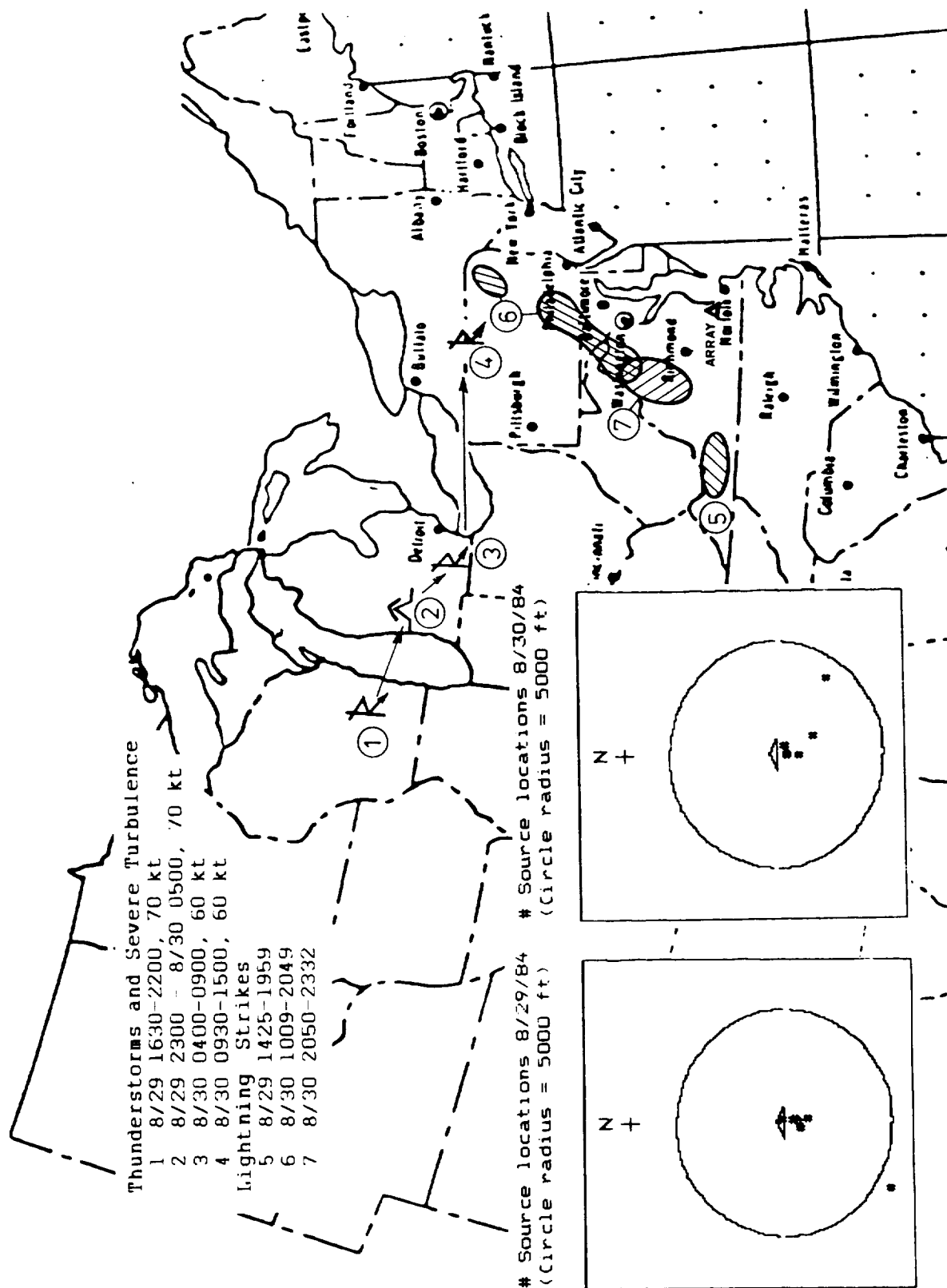


Figure 22.- Meteorological events and source locations (inserts) of August 29-30, 1984.

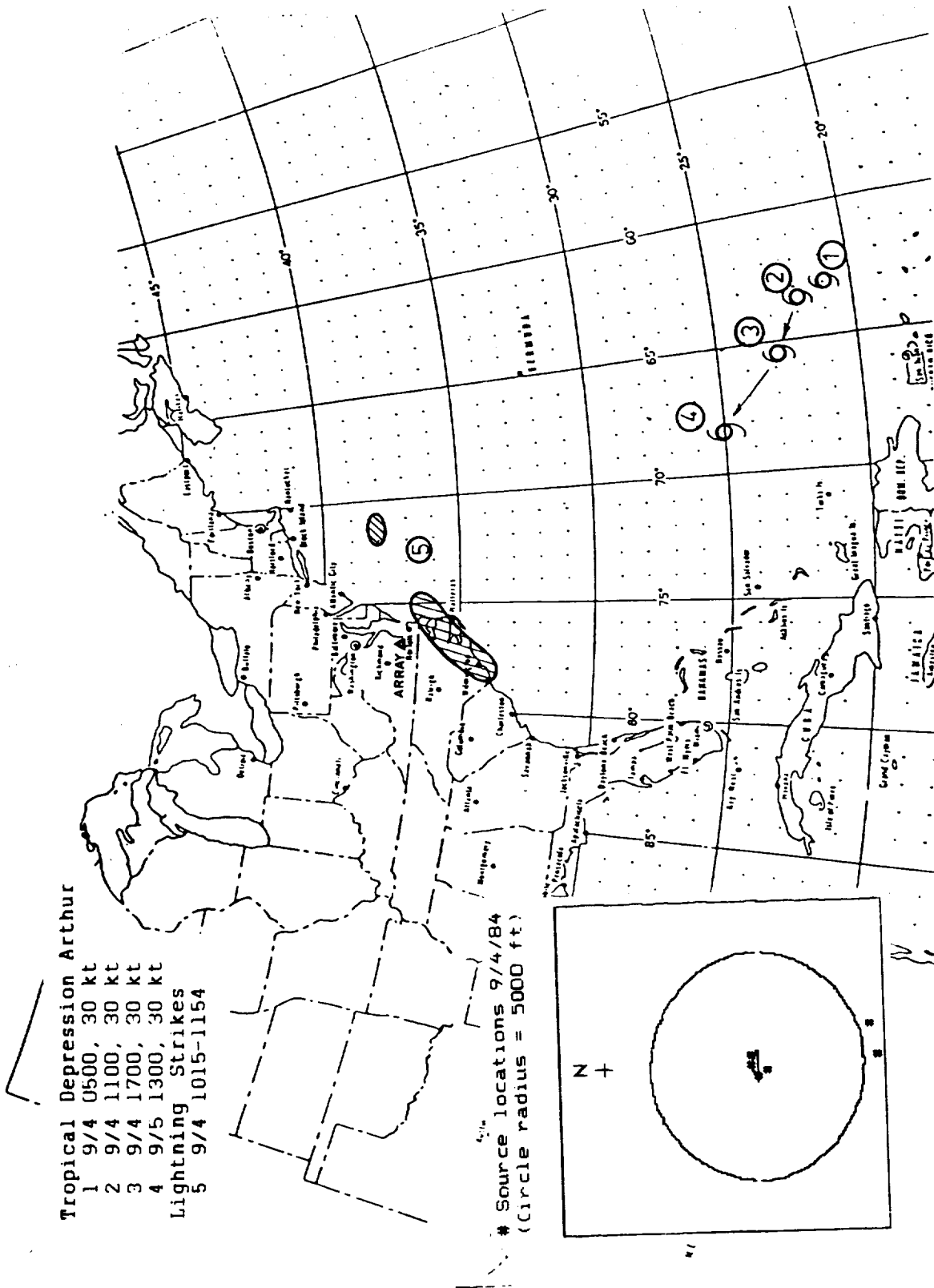


Figure 23.- Meteorological events and source locations (insert) of September 4, 1984.

ORIGINAL PAGE IS
OF POOR QUALITY

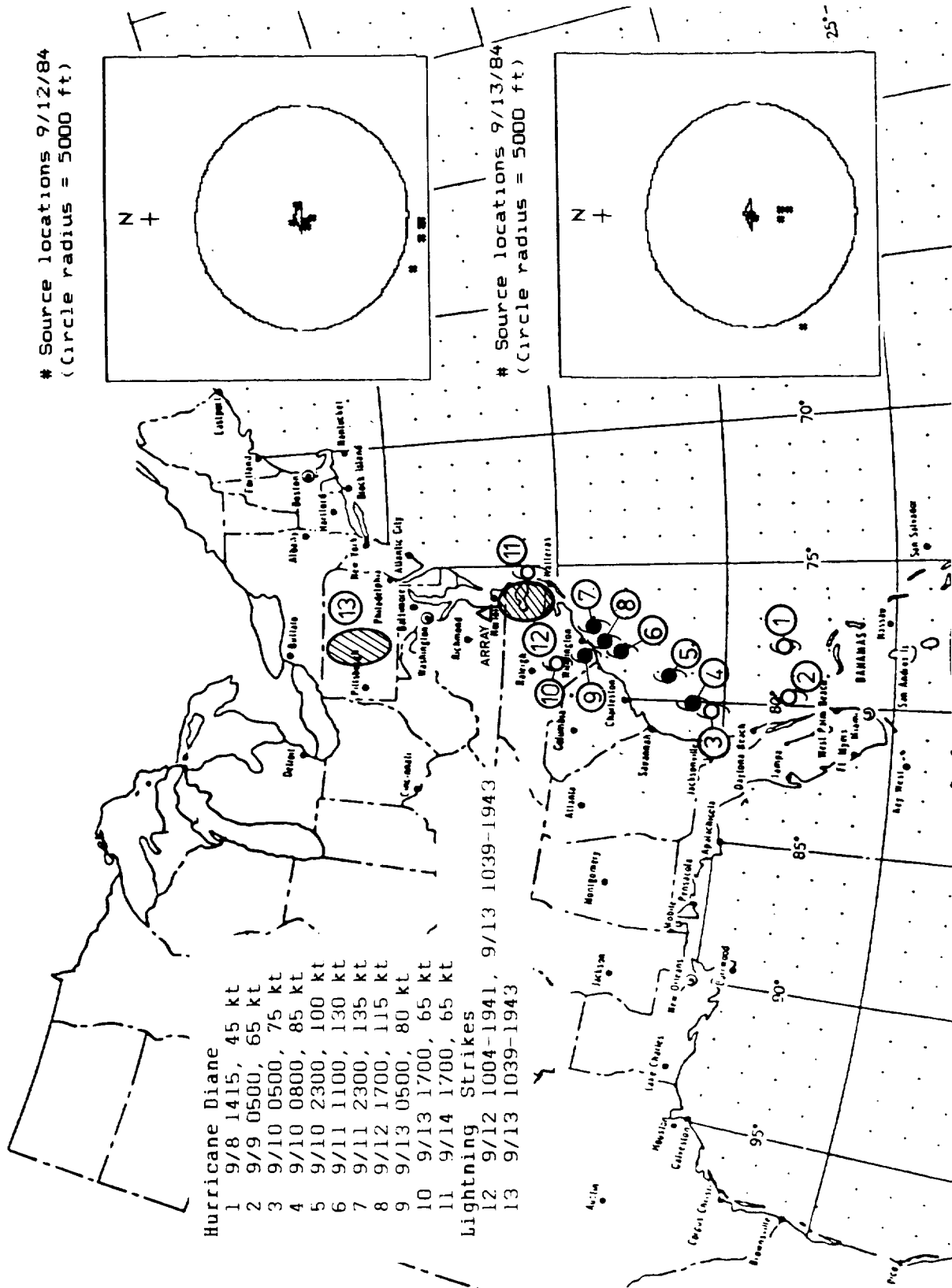


Figure 24.- Meteorological events and source locations (inserts) of September 12-13, 1984.

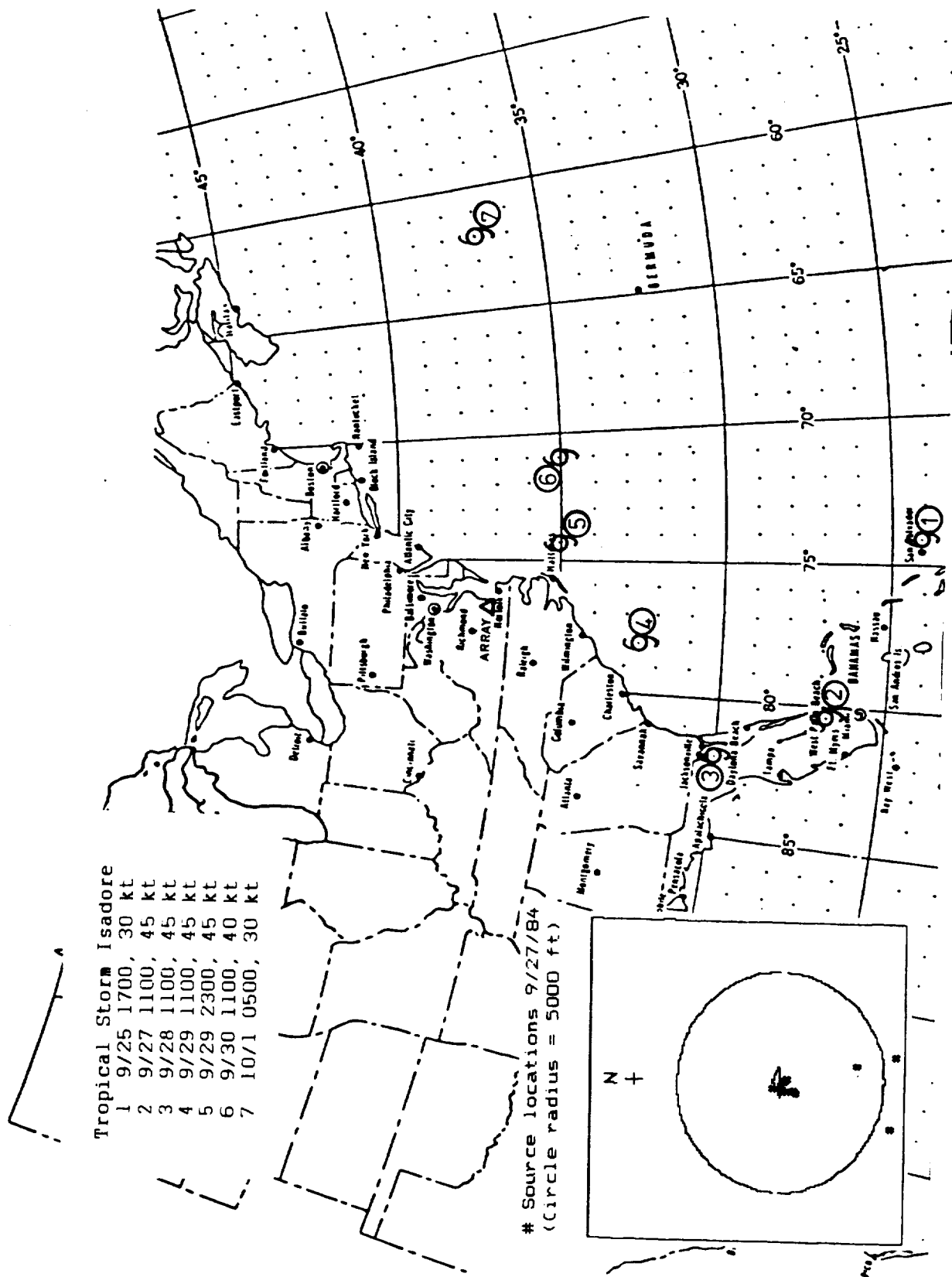


Figure 25.- Meteorological events and source locations (insert) of September 27-October 1, 1984.

ORIGINAL PAGE IS
OF POOR QUALITY

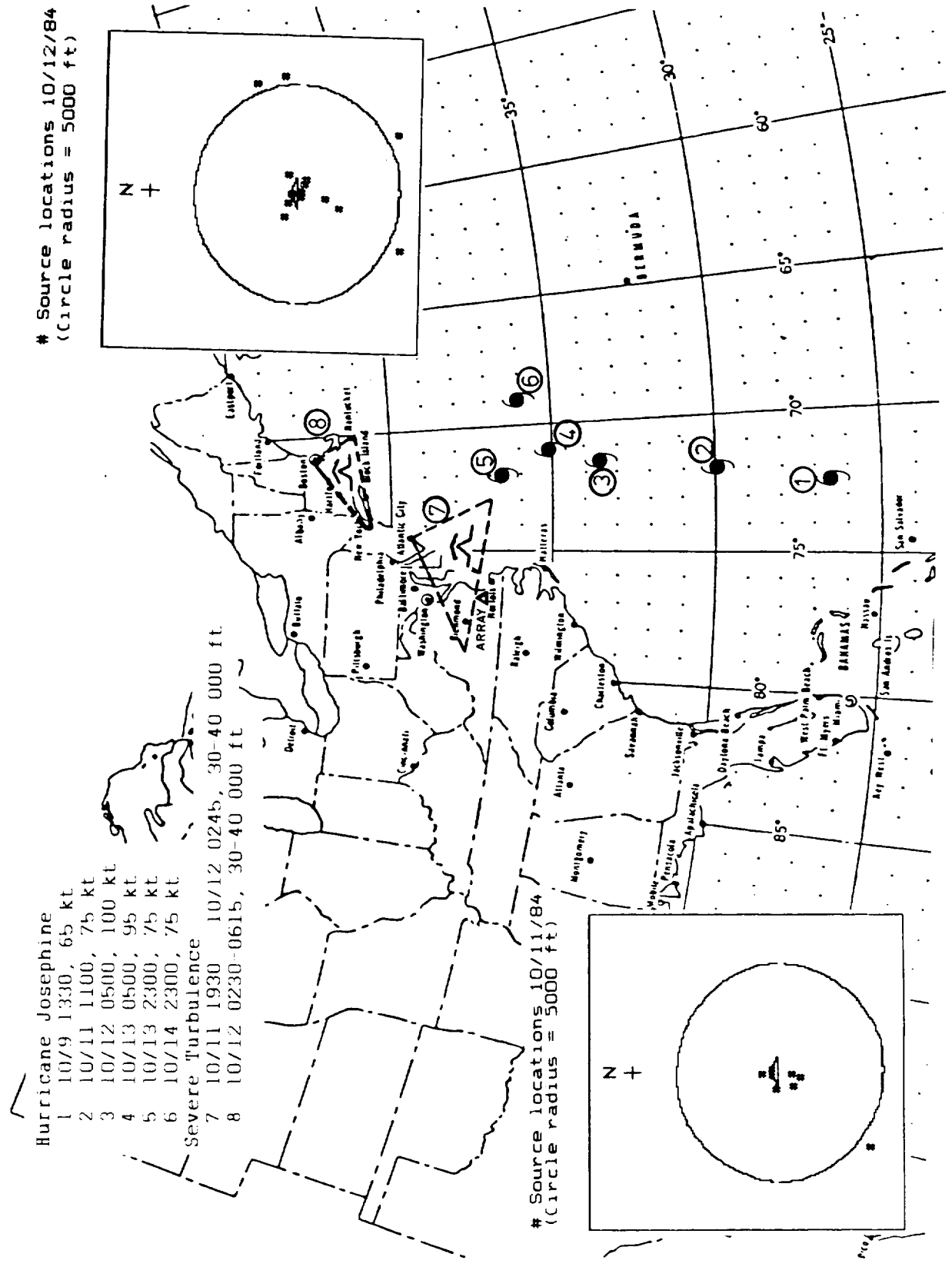


Figure 26.- Meteorological events and source locations (inserts) of October 11-12, 1984.

Severe Turbulence

- 1 11/2 0040, 24-40 000 ft
- 2 11/2 0000-1800, below 12 000 ft

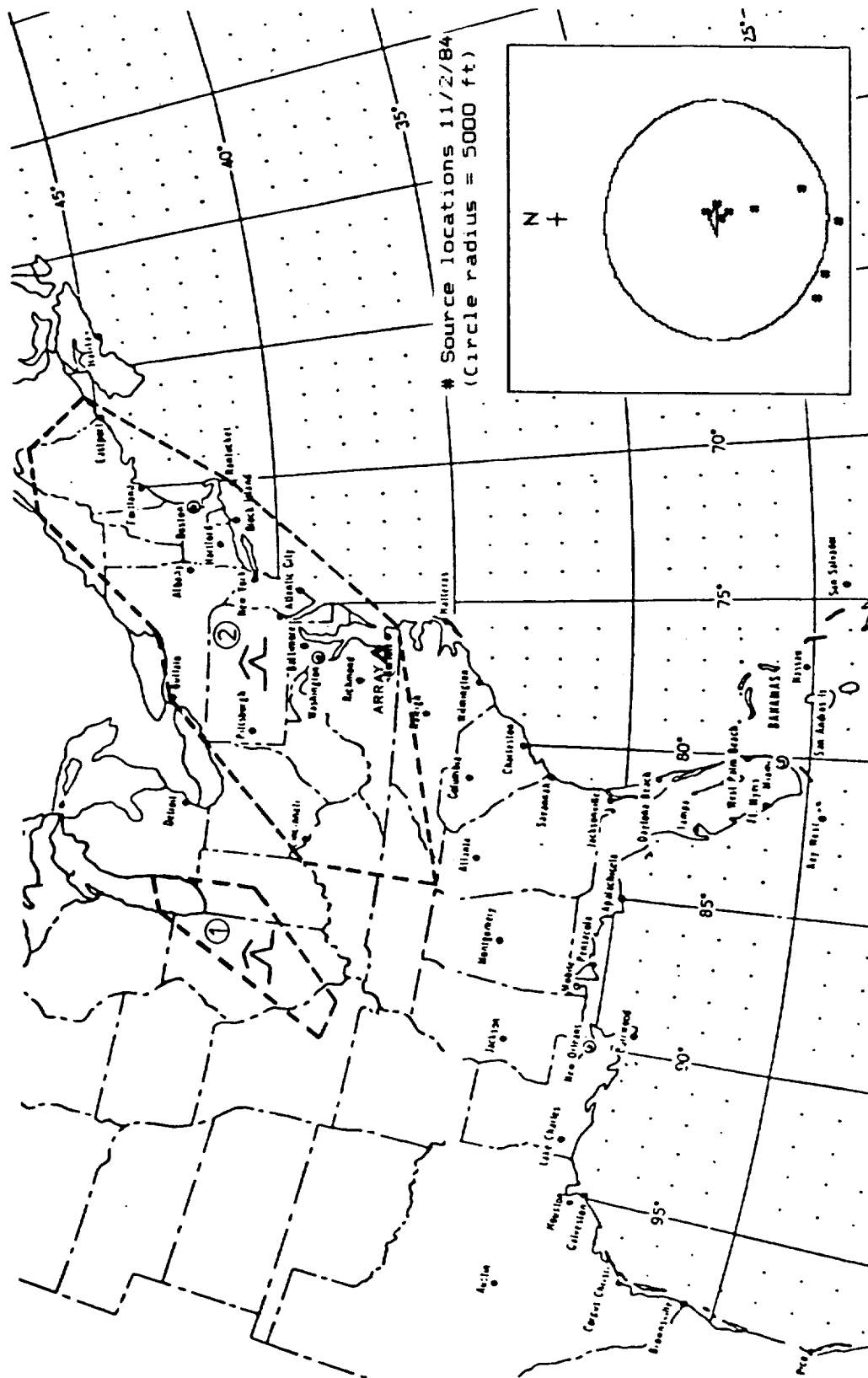


Figure 27.- Meteorological events and source locations (insert) of November 2, 1984.

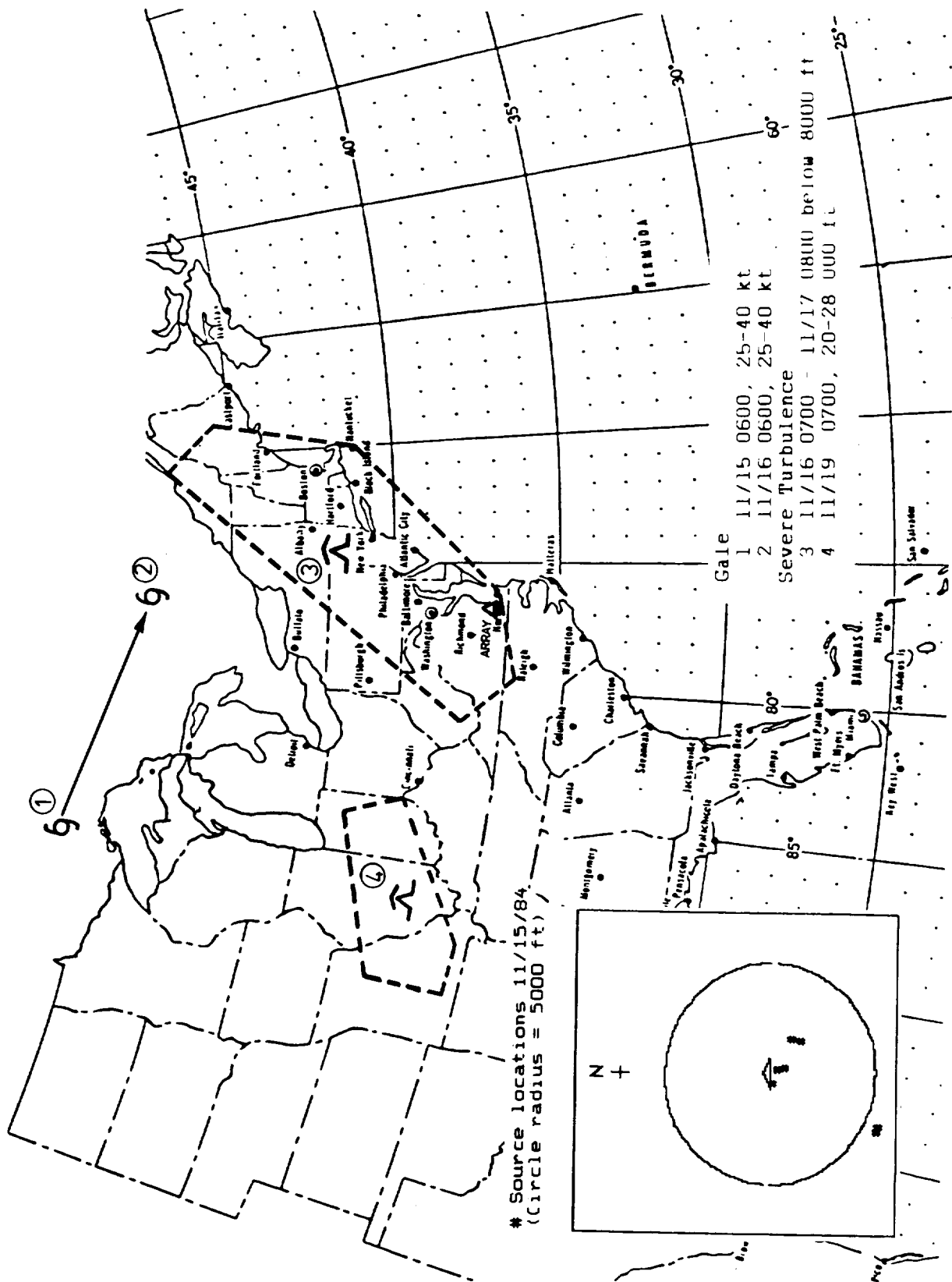


Figure 28.-- Meteorological events and source locations (insert) of November 15, 1984.

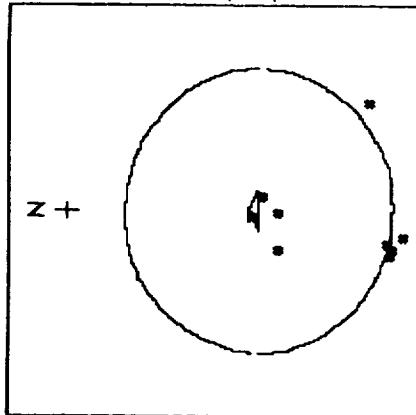
Gales

- 1 11/22 0000, 30-40 kt
- 2 11/22 1800, 30-40 kt
- 3 11/23 0600, 30-45 kt
- 4 11/24 0000, 25-35 kt
- 5 11/23 1200, 20-35 kt
- 6 11/24 0000, 30-45 kt
- 7 11/24 1200, 30-35 kt
- 8 11/25 0000, 30-45 kt

Severe Turbulence

- 9 11/21 2000-2400, 15-25 000 ft
- 10 11/22 1335-11/24 0345, below 8000 ft)

Source locations 11/20/84
(Circle radius = 5000 ft)



Source locations 11/23/84
(Circle radius = 5000 ft)

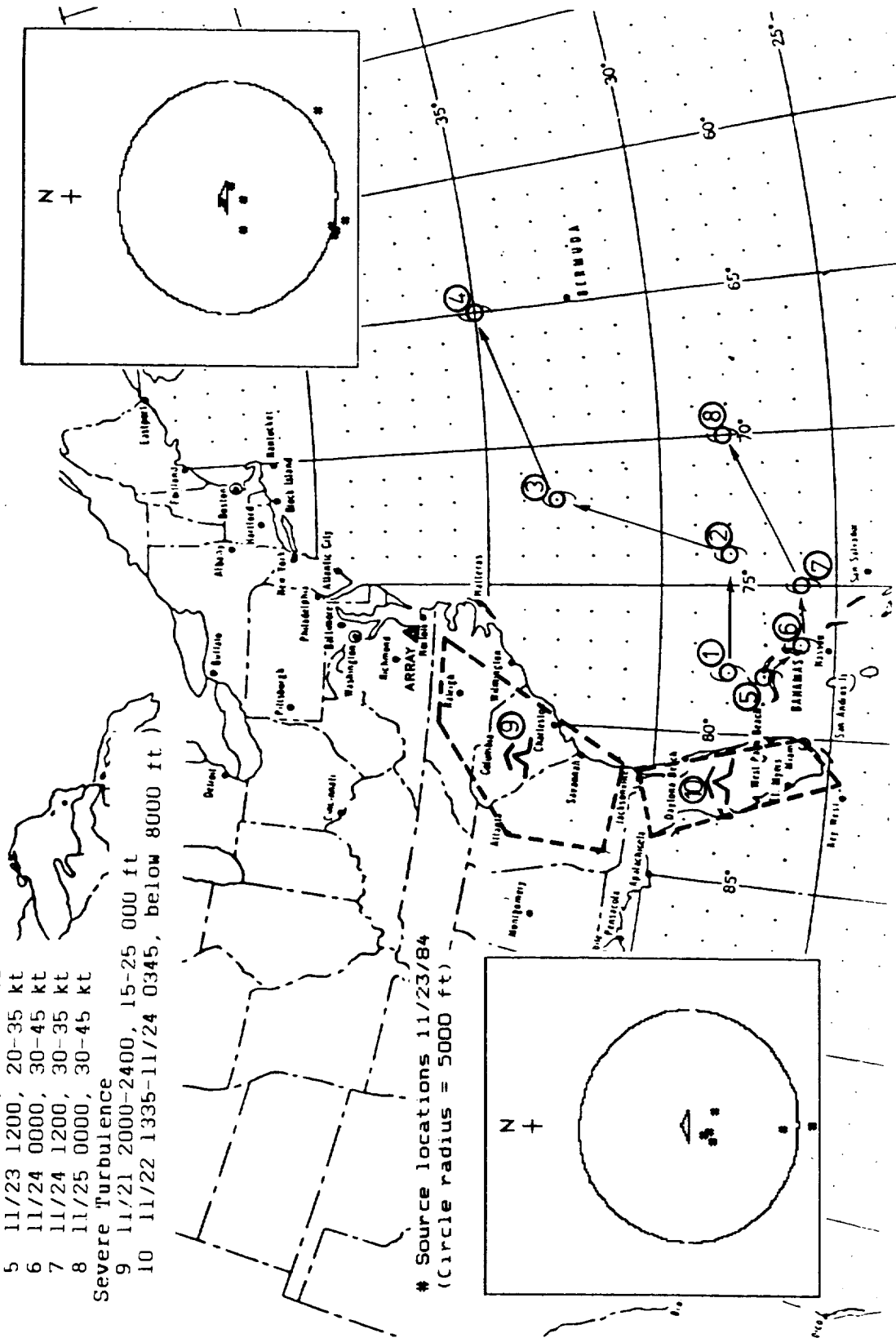
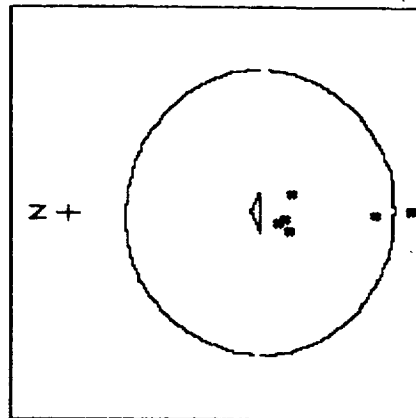


Figure 29.- Meteorological events and source locations (inserts) of November 20-24, 1984.

ORIGINAL PAGE IS
OF POOR QUALITY

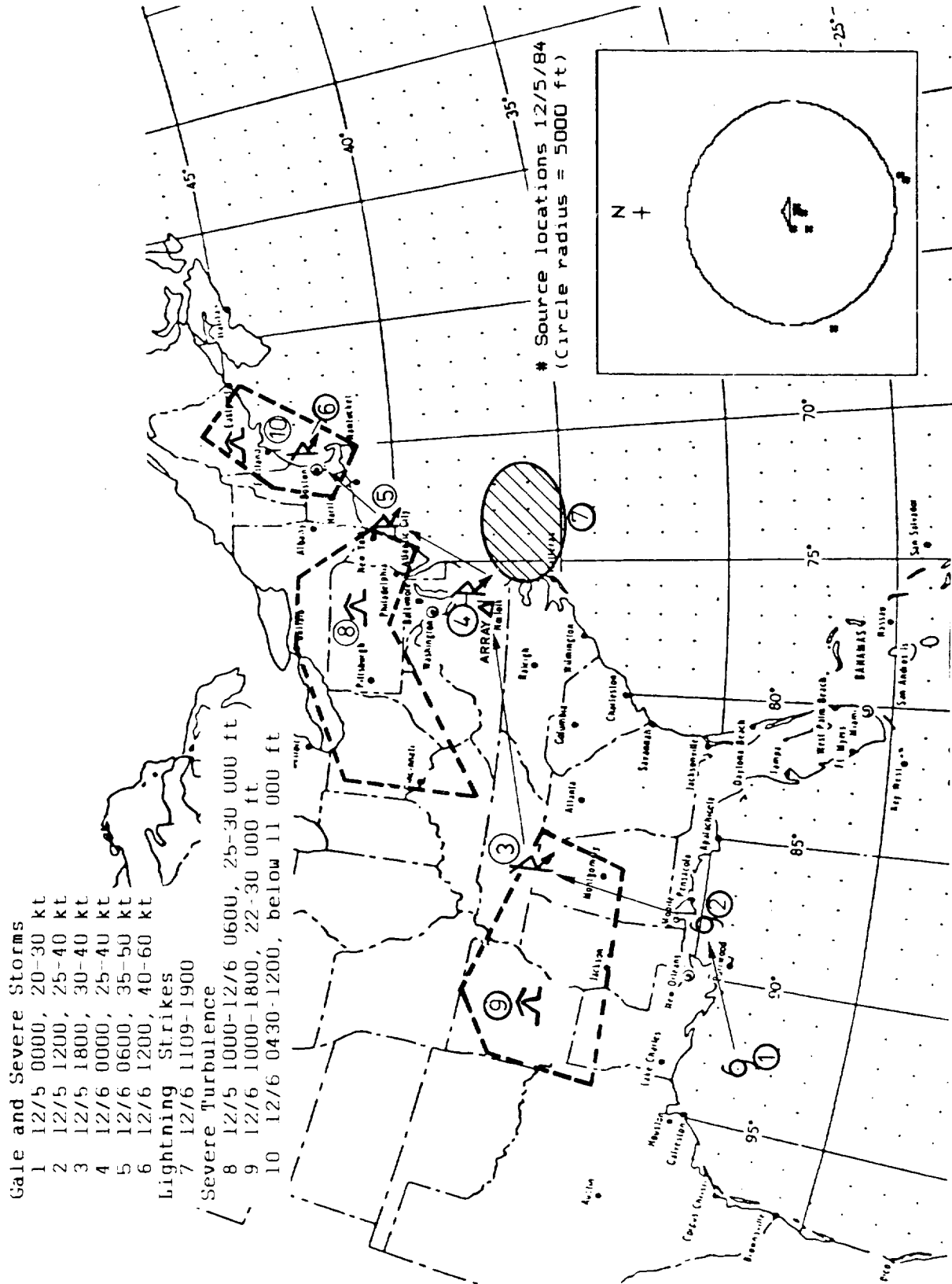


Figure 30.- Meteorological events and source locations (insert) of December 5, 1984.

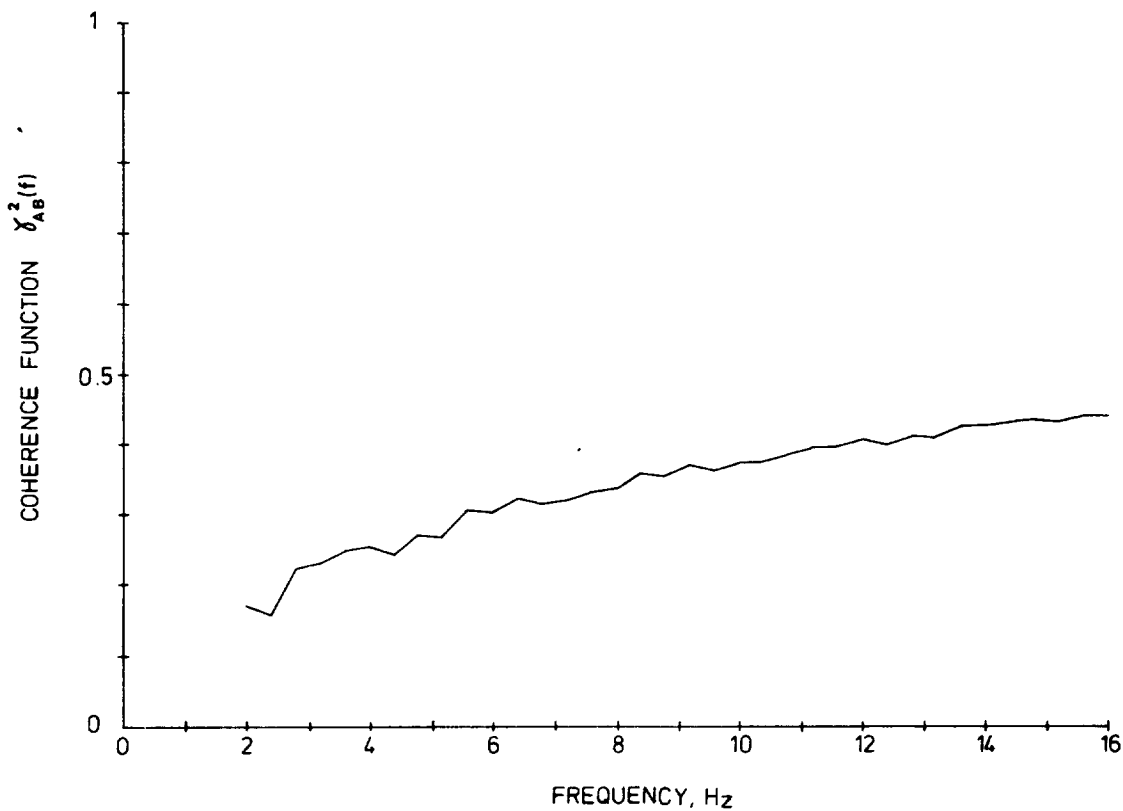


Figure 31.- Coherence function versus frequency computed from equation (7). The diffuse noise spectrum $G_d(f)$ is that of the top of figure 13, with parameter values $A_0 = 10^5$, $A_1 = 2.5$ [eq. (19)]. The coherent source spectrum has parameter values $B_0 = 5 \times 10^4$, $B_1 = 2.0$ [eq. (20)].

Standard Bibliographic Page

1. Report No. NASA TM-87686		2. Government Accession No.		3. Recipient's Catalog No.	
4. Title and Subtitle Infrasonic Emissions from Local Meteorological Events: A Summary of Data Taken Throughout 1984				5. Report Date February 1986	
				6. Performing Organization Code 141-30-30-01	
7. Author(s) Allan J. Zuckerwar				8. Performing Organization Report No.	
9. Performing Organization Name and Address NASA Langley Research Center Hampton, VA 23665-5225				10. Work Unit No.	
				11. Contract or Grant No.	
12. Sponsoring Agency Name and Address National Aeronautics and Space Administration Washington, DC 20546-0001				13. Type of Report and Period Covered Technical Memorandum	
				14. Sponsoring Agency Code	
15. Supplementary Notes					
15. Abstract Records of infrasonic signals, propagating through the Earth's atmosphere in the frequency band 2-16 Hz, were gathered on a three-microphone array at Langley Research Center throughout the year 1984. Digital processing of these records fulfilled three functions: time delay estimation, based on an adaptive filter; source location, determined from the time delay estimates; and source identification, based on spectral analysis. Meteorological support was provided by significant meteorological advisories, lightning locator plots, and daily reports from the Air Weather Service. The infrasonic data are organized into four characteristic signatures, one of which is believed to contain emissions from local meteorological sources (low level wind shear, microbursts, etc.). This class of signature prevailed only on those days when a major global meteorological event appeared in or near the eastern United States. Eleven case histories are examined. Practical application of the infrasonic array in a low level wind shear alert system is discussed.					
17. Key Words (Suggested by Authors(s)) Microbursts Infrasound Array Turbulence Meteorological Events				18. Distribution Statement Unclassified - Unlimited Subject Category - 71	
19. Security Classif.(of this report) Unclassified		20. Security Classif.(of this page) Unclassified		21. No. of Pages 49	
				22. Price A03	

For sale by the National Technical Information Service, Springfield, Virginia 22161

